SHELL BUCKLING – AN OVERVIEW

PART 1: The following is primarily from the 1981 "pitfalls" paper in the AIAA Journal: David Bushnell, "Buckling of shells – pitfall for designers", AIAA Journal, Vol. 19, No. 9, 1981 (see1981pitfalls.pdf), Presented as AIAA Paper 80-0665R, the SDM Lecture, at the AIAA/ASME/ASCE/AHS 21st Structures, Structural Dynamics and Materials Conference, Seattle, Washington, May12-14, 1980

BUCKLING OF SHELLS—PITFALL FOR DESIGNERS

David Bushnell, Lockheed Palo Alto Research Laboratory, Palo Alto, California

David Bushnell, b.1938 (photo taken in 1975)

David Bushnell joined Lockheed Missiles & Space Company, after receiving his B.S. and M.S. degrees in aerospace engineering from the Massachusetts Institute of Technology in 1961. In 1965, while at Lockheed, he earned his Ph.D. in Aeronautics and Astronautics at Stanford University. He then began extensive investigations of the stress, buckling and vibration behavior of thin shell structures. That work has resulted in over 40 papers and ultimately in the development of the BOSOR4 and BOSOR5 computer programs, widely used codes for the stress, buckling, and vibration analysis of shells of revolution. Many of the examples in this survey article are based on applications of these computer programs to practical problems involving complex shell structures. In 1975 Dr. Bushnell received the ONR/AIAA Structural Mechanics Research Award, the topic of his investigation being "Stress, Buckling, and Vibration of Hybrid Bodies of Revolution." He served as Associate Editor of the *AIAA Journal* from 1977 to 1979 and was a member of the AIAA Structures Technical Committee 1978 to 1979. Dr. Bushnell was elected the Outstanding Engineer of the AIAA San Francisco Chapter for the year 1978, and is an Associate Fellow of AIAA. (2011 NOTE: This biography was written in May, 1980)

1. Introduction (2011 Note: for references and more detail, see 1981pitfalls.pdf)

Purpose

In order to produce efficient, reliable designs and to avoid unexpected catastrophic failure of structures of which thin shells are important components, the engineer must understand the physics of shell buckling. The objective of this survey is to convey to the reader a "feel" for shell buckling, whether it is due to nonlinear collapse, bifurcation buckling, or a combination of these modes. This intuitive understanding of instability is communicated by a large number of examples involving practical shell structures that may be stiffened, segmented, or branched and which have complex wall constructions. With such intuitive knowledge the engineer will have an improved ability to foresee situations in which buckling might occur and to modify a design to avoid it. He or she will be able to set up more appropriate models for tests and analytical predictions. The emphasis here is not on the development of equations for the prediction of instability. For such material the reader is referred to the book by Brush and Almroth [11]. (2011 note: Also see and download the files, 1981pitfalls.refs.pdf and 1996bucklingsurvey.pdf and shellbucklingrefs.pdf.)

Emphasis is given here to nonlinear behavior caused by a combination of large deflections and plasticity. Also illustrated are stress redistribution effects, stiffener and load path eccentricity effects, local versus general instability, imperfection sensitivity, and modal interaction in optimized structures. Scattered throughout the text are tips on modeling for computerized analysis. The survey is divided into nine major sections describing: 1) several examples of catastrophic failure of expensive shell structures; 2) the basics of buckling behavior; 3) "classical" buckling and imperfection sensitivity; 4) nonlinear collapse and the appropriateness of linear bifurcation buckling analyses for general shells; 5) bifurcation buckling with significant nonlinear pre-buckling behavior; 6) effects of boundary conditions, load eccentricity, transverse shear deformation, and stable post-buckling behavior; 7) optimization of buckling-critical structures with consequent modal interaction; 8) a suggested design method for axially compressed cylinders with stiffeners, internal pressure or other special characteristics; and 9) two examples in which sophisticated buckling analyses are required in order to derive improved designs. The paper focuses on static buckling problems. (2011 NOTE: Download the file,

1981pitfalls.pdf and the PowerPoint slide show, pitfallsnasa.ppt .)

Fig. 1.1 Buckling is a somewhat mystifying phenomenon (courtesy of St. Regis Paper Company). (from AIAA Journal, Vol. 19, No. 9, 1981)

2. Some Buckling Basics

Why Do Shells Buckle?

The property of thinness of a shell wall has a consequence that is pointed out in Ref. 14: The membrane stiffness is in general several orders of magnitude greater than

the bending stiffness. A thin shell can absorb a great deal of membrane strain energy without deforming too much. It must deform much more in order to absorb an equivalent amount of bending strain energy. If the shell is loaded in such a way that most of its strain energy is in the form of membrane compression, and if there is a way that this stored-up membrane energy can be converted into bending energy, the shell may fail rather dramatically in a process called "buckling" as it exchanges its membrane energy for bending energy. Very large deflections are generally required to convert a given amount of membrane energy into bending energy. The way in which buckling occurs depends on how the shell is loaded and on its geometrical and material properties. The pre-buckling process is often nonlinear if there is a reasonably large percentage of bending energy being stored in the shell throughout the loading history.

What is Buckling?

To most laymen the word "buckling" evokes an image of failure of a structure that has been compressed in some way. Pictures and perhaps sounds come to mind of sudden, catastrophic collapse involving very large deformations, such as those displayed below by Falstaff's boots (picture added, 2011).

Falstaff's boots have experienced two types of buckling:

1. axisymmetric collapse (the top part of Falstaff's left boot), and

2. non-axisymmetric bifurcation buckling and post-bifurcation deformation (lower down in both boots). (from the pitfallsnasa.ppt file)

From a scientific and engineering point of view, the interesting phases of buckling phenomena generally occur before the deformations are very large, when to the unaided eye the structure appears to be undeformed or only slightly deformed. In the static analysis of perfect structures, the two phenomena loosely termed "buckling" are:

(1) collapse at the maximum point in a load versus deflection curve, and

(2) bifurcation buckling.

To use a more “classical” engineering example than Falstaff’s boots, these two types of instability failure are illustrated again in Figs. 2.1 and 2.2.

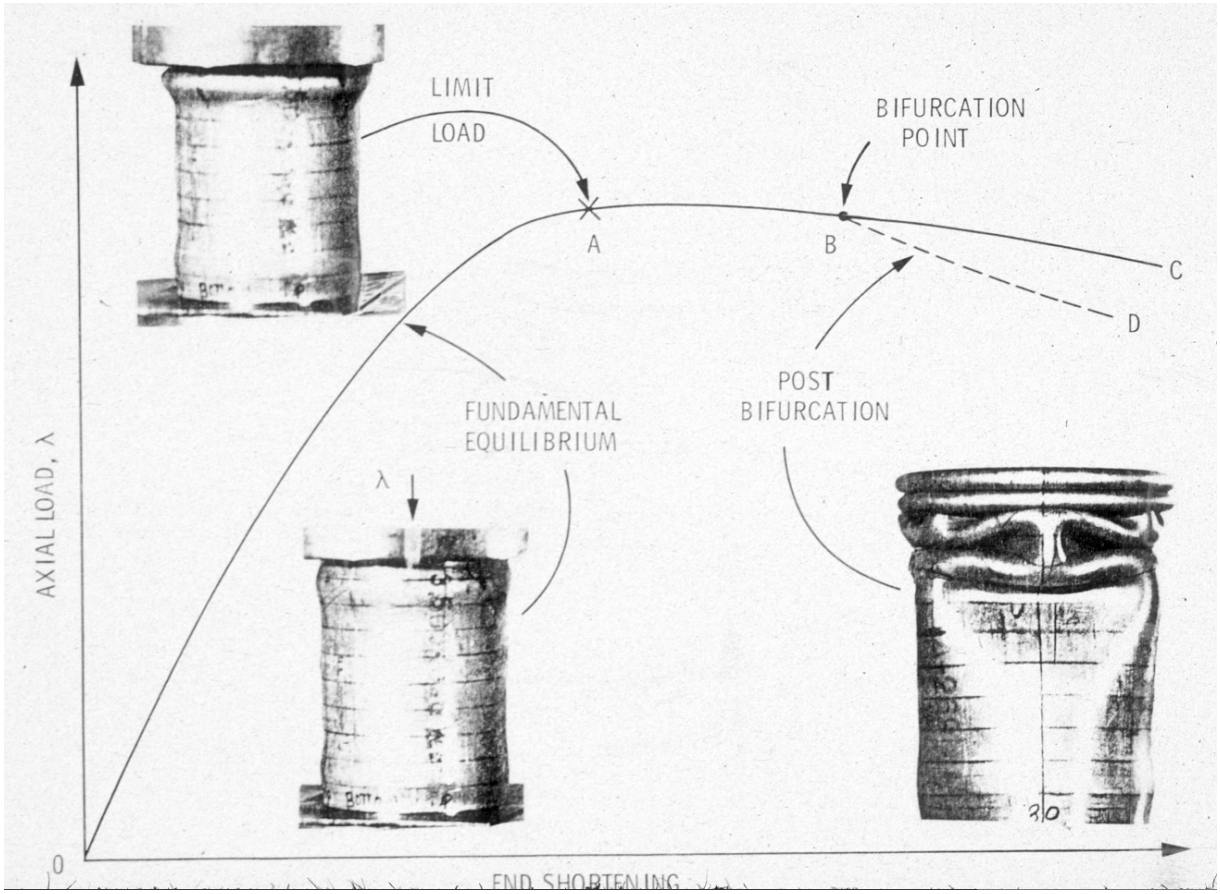

Fig. 2.1 Load/end-shortening curve with collapse load A, bifurcation point B, and post-bifurcation equilibrium path BD (photographs courtesy of Sobel and Newman [87]). (from AIAA Journal, Vol. 19, No. 9, 1981)

The rather thick axially compressed cylinder shown in Fig. 2.1 deforms approximately axisymmetrically along the equilibrium path OA until a maximum or collapse load $lambda_A$ is reached at point A. If the axial load, lambda, is not sufficiently relieved by the reduction in axial stiffness, the perfect cylindrical shell will fail at this collapse load, following either path ABC along which it continues to deform axisymmetrically (the path followed by the top part of Falstaff's left boot) or some other path ABD along which it first deforms axisymmetrically from A to B and then non-axisymmetrically from B to D (the path taken by the lower parts of both of Falstaff's boots).

Nonlinear buckling or "snap-through" occurs at point A and bifurcation buckling at point B. The equilibrium path OABC, corresponding to the symmetric mode of deformation, is called the fundamental or primary or pre-buckling equilibrium path. The post-bifurcation equilibrium path BD, corresponding to the non-axisymmetric mode of deformation, is called the secondary or post-buckling path. Buckling of either the collapse or bifurcation type may occur at loads for which some or all of the structural material has been stressed beyond its proportional limit. The example in Fig. 2.1 is somewhat unusual in that the bifurcation points B is shown to occur after the collapse point has been reached. In this particular case, therefore, bifurcation buckling is of less engineering significance than axisymmetric collapse.

A perhaps more commonly occurring situation is illustrated in Fig. 2.2a.

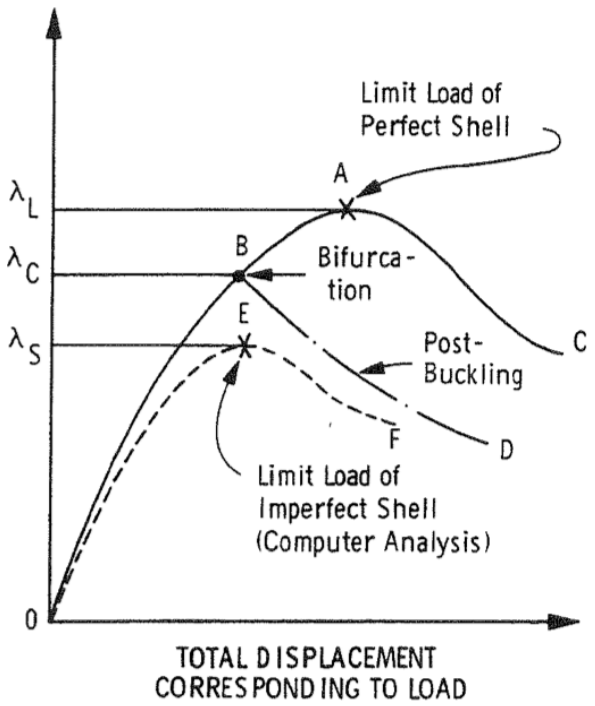

Fig. 2.2(a) Load-deflection curves showing limit and bifurcation points. The load at which the structure represented by these curves fails is mildly sensitive to initial imperfections because the point E is not too far below the point B, which pertains to the perfect shell. (from AIAA Journal, Vol. 19, No. 9, 1981)

The bifurcation point B is between 0 and A. If the fundamental path OAC corresponds to axisymmetric deformation and BD to non-axisymmetric deformation, the initial failure of the structure represented by these paths would generally be characterized by rapidly growing non-axisymmetric deformations. In this case the collapse load of the perfect structure, $Lambda_L$, is of less engineering significance than the bifurcation point, $Lambda_C$.

The next figure (not shown in the 1981 "Pitfalls" paper) is analogous to Fig. 2.2a. This sketch represents the behavior of a structure that is extremely "imperfection sensitive", that is, the load at which the structure fails is extremely sensitive to initial imperfections because the load-bearing capacity of the imperfect structure (peaks of the two curves labeled "Imperfect shell") is far below the point B, the load-bearing capacity of the perfect shell. (See imperfection sensitivity).

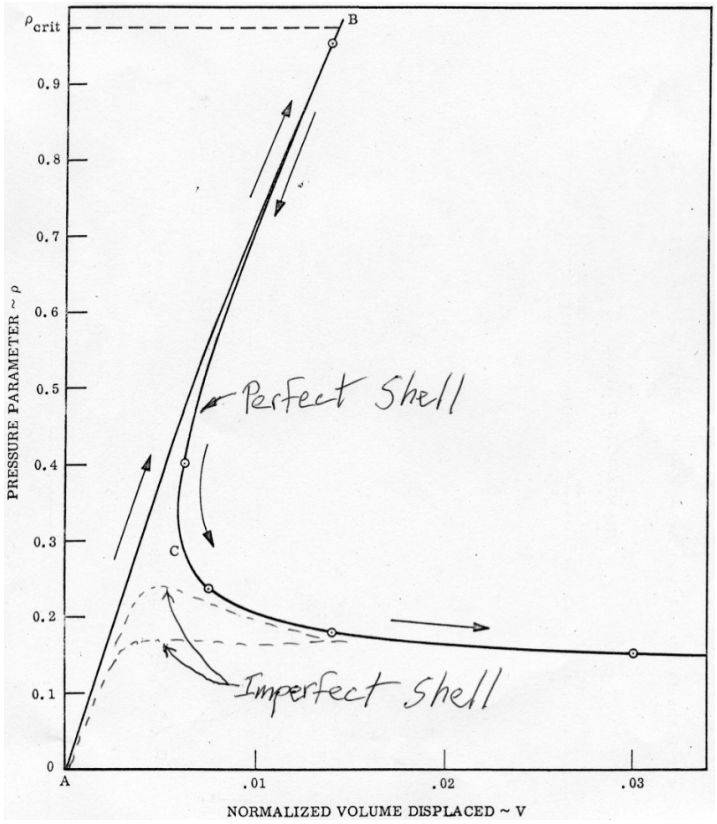

This figure shows the behavior of a very thin cylindrical shell under uniform compression or a very thin spherical shell under uniform external pressure. Again, the same physics and mathematics applies as in the previous two figures. However, in this case there is a dramatic effect of an initial imperfection on the load-carrying capacity of the shell. (from the pitfallsnasa.ppt file)

In the case of real structures that contain unavoidable imperfections, there is no such thing as true bifurcation buckling. The actual structure will follow a fundamental path OEF in Fig. 2.2a, with the failure corresponding to the"snap-through"at point E at the collapse load, $Lambda_S$. If point B in Fig. 2.2a corresponds to bifurcation into a non-axisymmetric buckling mode, the collapse at E will involve significant non-axisymmetric displacement components. Although true bifurcation buckling is fictitious, the bifurcation buckling analytical model is valid in that it is computationally convenient and economical and often leads to a good approximation of the actual failure load and mode shape.

Various Types of Bifurcation Buckling

In Fig. 2.2b the load is plotted as a function of amplitude of the bifurcation buckling mode. The pre-buckling load path of the perfect shell is represented by the path OB. Since the bifurcation buckling mode is orthogonal to the pre-buckling

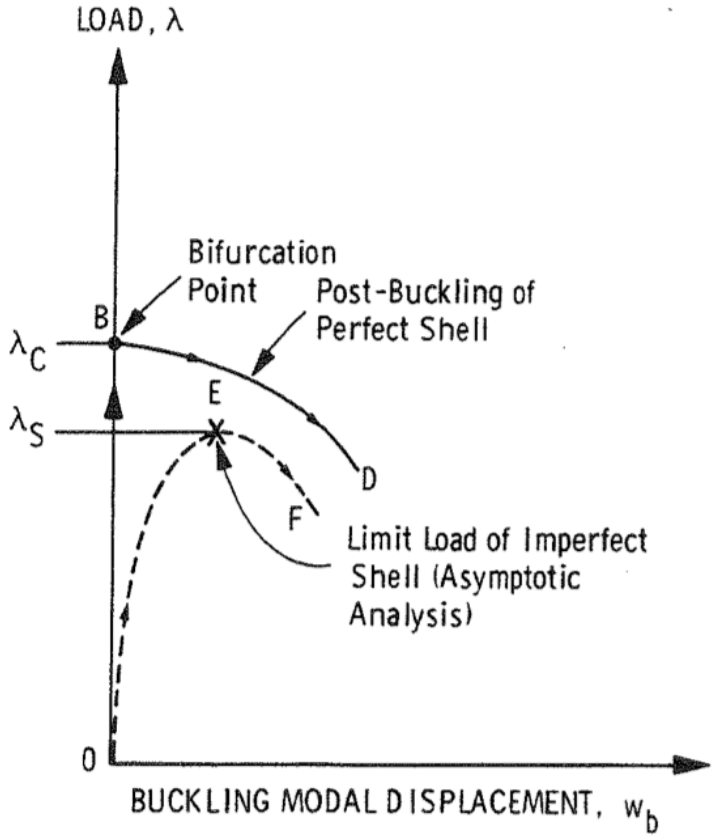

Fig. 2.2(b) Load-deflection curves showing limit and bifurcation points: Asymptotic analysis. (from AIAA Journal, Vol. 19, No. 9, 1981)

displacement pattern of the perfect shell, its amplitude remains zero until the bifurcation point B is reached. The curve BD in Fig. 2.2b implies that the post-buckling state is unstable: the load-carrying capability, Lambda, decreases with increasing amplitude of the bifurcation buckling mode.

All real structures are imperfect. The imperfection shape is, in general, not orthogonal to the bifurcation buckling mode. If one expressed the deformation of the imperfect structure as a sum of two components, the fundamental pre-buckling equilibrium state of the perfect structure plus the bifurcation buckling mode of the perfect structure (presumed here to be unique), then one would obtain the curve OEF in Fig. 2.2b if one plotted the amplitude of the bifurcation modal component versus the load for the imperfect structure. The amplitude of the bifurcation modal component would increase at an increasing rate until instability via nonlinear "snap-through" or collapse would occur at the reduced load, $Lambda_S$. The difference between the critical bifurcation load, $Lambda_C$, of the perfect structure and the collapse load, $Lambda_S$, of the imperfect structure depends on the amplitude of the

initial imperfection, call it w_{b0}. A chart of $\text{Lambda}_S/\text{Lambda}_C$ versus w_{bo} would characterize the sensitivity of the maximum load, Lambda_S, to initial geometrical imperfections. According to the jargon that has become accepted over the years, the structure to which the curves in Fig. 2.2b correspond is called "imperfection sensitive" because imperfections reduce its maximum load-carrying capability. (Of course, it is not the *structure* that is sensitive to imperfections, but the maximum *load* it can safely support!) (2011 Note: for more on "imperfection sensitivity" see the "page", imperfection sensitivity.)

Not all structures or mathematical models of them behave as shown in Fig. 2.2b. Figure 2.3 shows various types of post-buckling behavior. A linearized model of elastic stability, that is, an eigenvalue formulation of the buckling problem, implies a load-deflection behavior shown in Fig. 2.3a: The amplitude of the eigenvector, the bifurcation buckling mode, is indeterminate, which implies that the load, Lambda, remains constant: $\text{Lambda} = \text{Lambda}_C$ with increasing buckling modal deflection, w_b. The equilibrium path for the slightly imperfect structure follows the rectangular hyperbolic path,

$$\boldsymbol{w_b = w_{bo}}/(\text{Lambda}_C/\text{Lambda} - 1) \qquad (1)$$

shown as a dotted line in Fig. 2.3a.

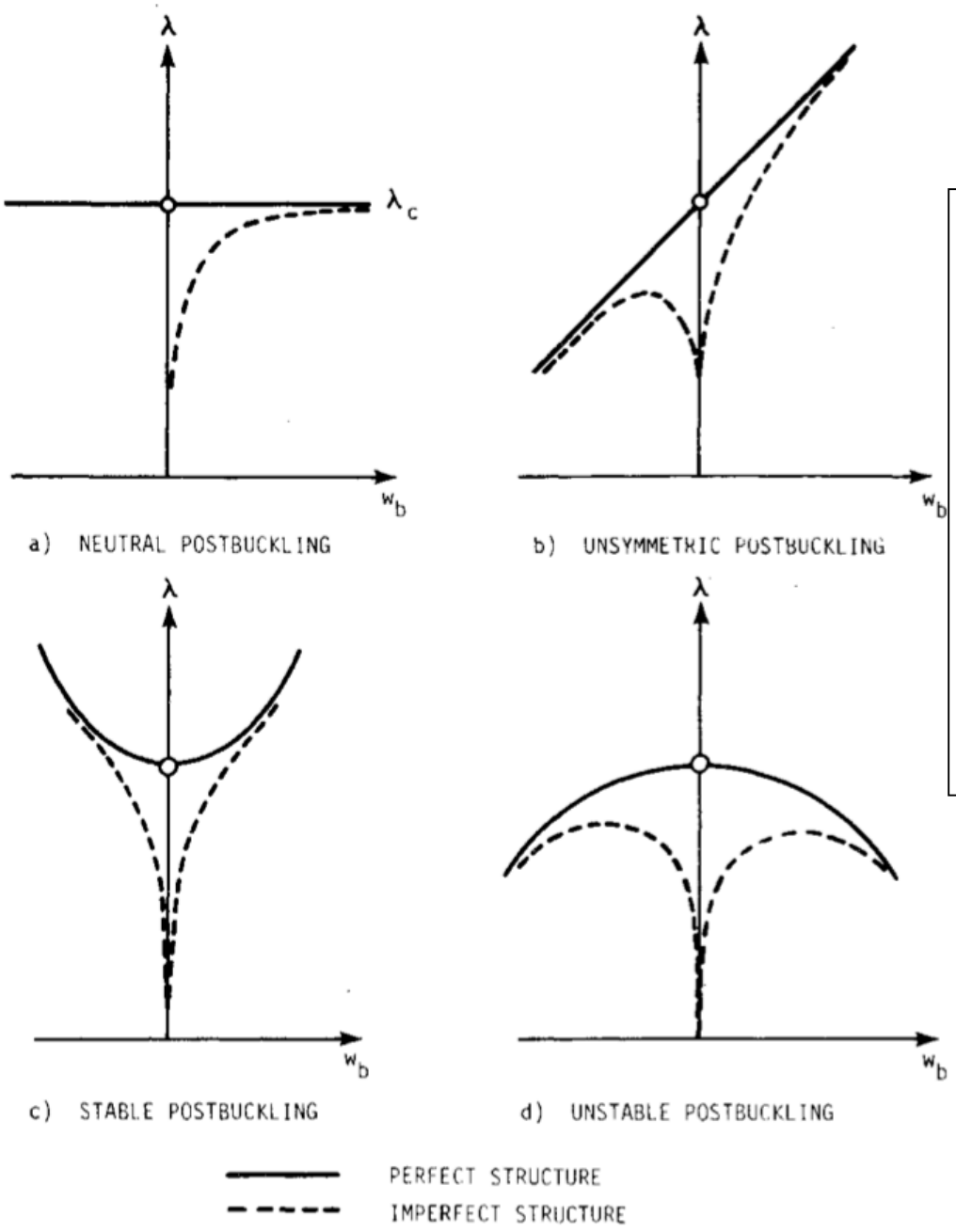

Fig. 2.3 Different types of post-buckling load-displacement relations (Lambda is the load; w_b is the amplitude of the buckling modal displacement). (from AIAA Journal, Vol. 19, No. 9, 1981)

If nonlinear post-buckling effects are accounted for, equilibrium paths for most structures have the forms shown in Figs. 2.3b-d. The asymmetric nature of the curves in Fig. 2.3b indicates that the structure continues to carry loads above the bifurcation load, Lambda_C, if it is forced to buckle one way, but collapses if allowed to buckle the other. An example of this type of behavior is given by a structure with parts that move relative to each other as buckling proceeds in such a way that these

parts come in contact and support each other for positive deflections but move away from each other and form gaps for similar negative deflections. Specifically, a built-up panel consisting of a flat sheet riveted to a corrugated sheet is such a structure.

Roorda [15] has demonstrated this asymmetric post-buckling behavior for perfect and imperfect frames with eccentric loads. His results are summarized in [11]. The symmetric stable post-buckling behavior displayed in Fig. 2.3c is typical of axially compressed columns and isotropic flat plates. The perfect column or plate loaded precisely in its neutral axis or surface buckles either way with equal ease and the post-buckled equilibrium state is neutrally stable for very, very small w_b, becoming stable for larger w_b. The symmetric unstable post-buckling behavior shown in Fig. 2.3d is typical of the early post-bifurcation regimes of axially compressed thin cylindrical shells and externally pressurized thin spherical shells.

Capsule of Recent Progress in Buckling Analysis (modified in 2011)

Recent progress in our capability to predict buckling failure can be categorized into three main areas:

1) Development of asymptotic post-buckling theories and applications of these theories to specific classes of structures, such as simple plates, shells, and panels [16 – 18]. (2011 Note: for references see the paper, 1981pitfalls.pdf .)

2) Development of special-purpose computer programs for limit-point axisymmetric buckling and non-axisymmetric bifurcation buckling of axisymmetric structures [9, 22 – 24]. (See BIGBOSOR4, BOSOR5).

3) Development of general-purpose computer programs for calculation of static and dynamic behavior of structures, including large deflections, large strains, and nonlinear material effects [19 – 21]. (See STAGS)

Asymptotic Analysis

The asymptotic analyses surveyed in [16 – 18] rest on theoretical foundations

established by Koiter [25], whose general elastic post-bifurcation theory leads to an expansion for the load parameter, called Lambda (Figs. 2.2b and 2.3), in terms of the buckling modal amplitude w_b which is valid in the neighborhood of the critical bifurcation point in (Lambda, w_b) space. Figure 3.3 is an example. (In Fig. 3.3 the load, Lambda, is now called P, the buckling modal amplitude w_b is now called delta, and the limit load, Lambda_S is now called P_S.) The primary aims of the asymptotic analyses are to calculate the maximum loads for perfect and imperfect structures. These analyses have contributed vital physical insights into the buckling process and the effect of structural or loading imperfections on this process.

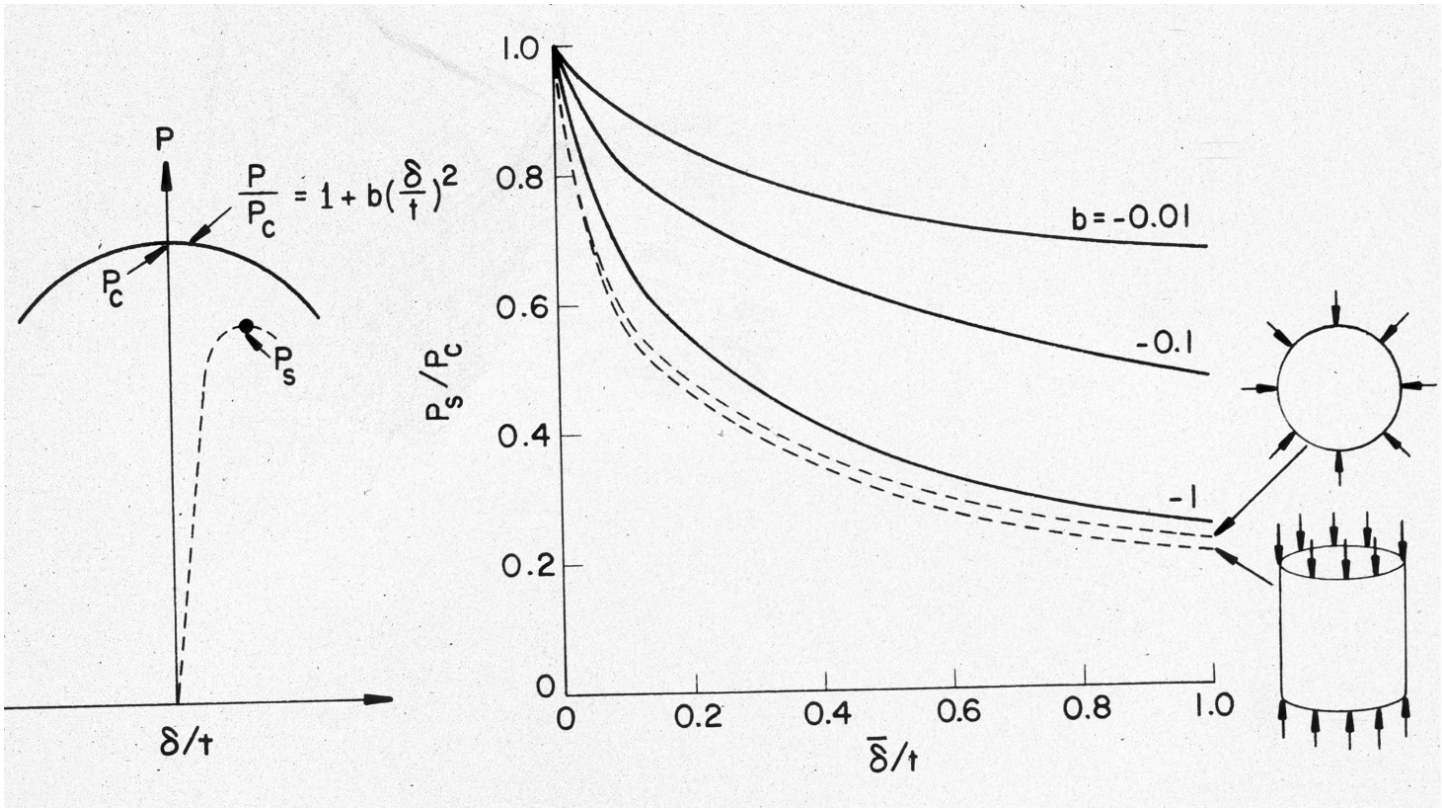

Fig. 3.3 Imperfection sensitivity as a function of the Koiter parameter **b** for a unique buckling mode, and comparison with the imperfection sensitivity of a spherical shell under external pressure and a cylindrical shell under axial compression. P_C is the buckling load of the perfect shell; delta is the amplitude of the buckling mode, deltabar is the amplitude of an imperfection in the shape of the critical buckling mode, and **t** is the shell wall thickness. (from Budiansky and Hutchinson [53]).

Axisymmetric Structures

The second approach to the buckling problem, development of special-purpose programs for the analysis of axisymmetric structures such as that displayed below (not included in the 1981 “Pitfalls” lecture), forms a sort of middle ground between

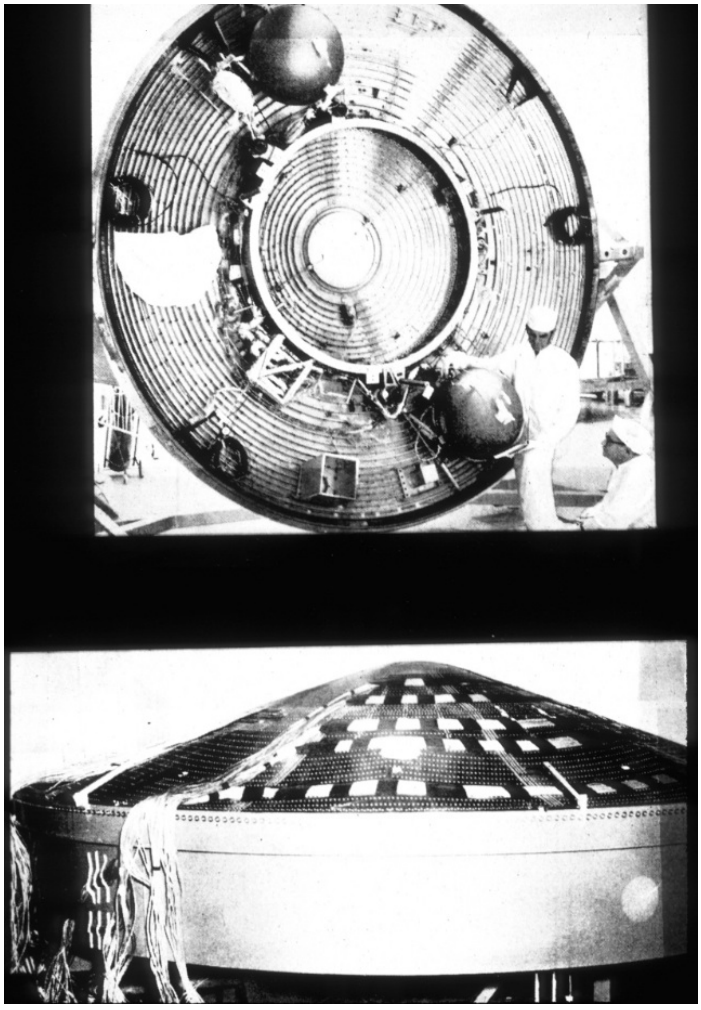

Buckling of an axisymmetric shell: a ring-stiffened shallow conical shell used for entry into the Martian atmosphere, tested at NASA Langley Research Center and analyzed by G. A. Cohen. (Cohen, G.A., "User Document for Computer Programs for Ring-Stiffened Shells of Revolution," NASA CR-2086, 1973; "Computer Analysis of Ring-Stiffened Shells of Revolution," NASA CR-2085, 1973; "Computer Program for Analysis of Imperfection Sensitivity of Ring-Stiffened Shells of Revolution," NASA CR-1801, 1971.) Photographs by Leonard, Anderson, and Heard, NASA Langley Research Center, 1974.

the asymptotic analysis and the general-purpose nonlinear analysis. The approach is similar to the asymptotic treatment because in applications it is restricted in practice to a special class of structures, and the distinction between pre-buckling equilibrium and bifurcation buckling is retained. It is similar to the general nonlinear approach in that the continuum is discretized and the nonlinear pre-buckling equilibrium problem is solved by "brute force." The emphasis is on the calculation of the pre-

buckling fundamental path, OB or OA in Fig. 2.2a and determination of the bifurcation point B and its associated buckling mode, not on calculation of post-bifurcation behavior BD or of the load-deflection path OEF of the imperfect structure. The goals of this second approach are to create an analysis tool for use by engineers and designers and to use this tool in extensive comparisons with tests, both to verify and to obtain physical insight into the buckling process. (2011 Note: See BIGBOSOR4 and BOSOR5.)

General Nonlinear Analysis (2011 Note: See STAGS.)
The general-purpose computer programs in widespread use since the early 1970s and presently being written are based on principles of continuum mechanics established for the most part by the late 1950s and set forth in several texts [26 – 31]. (2011 Note: For the references see 1981pitfalls.pdf.)

The structural continuum is discretized into finite elements as described in the texts [32 – 35], and various strategies are employed to solve the resulting nonlinear problem [19]. The nonlinearity is due to moderately large or very large deflections and nonlinear material behavior. Various plasticity models are described in texts, conference proceedings, and survey articles identified in [19].

The primary aim of this vast body of work, much of which was done in the1970s, has been to produce reliable analysis methods and computer programs for use by engineers and designers. Thus, the emphasis in the literature just cited is not primarily on the acquisition of new physical insight into buckling and post-bifurcation phenomena, but on the creation of tools that can be used to determine the equilibrium path OEF in Fig. 2.2a for an arbitrary structure and on proof that these tools work by the use of demonstration problems, the solution of which is known.

In most cases, no formal distinction is made between pre-bifurcation and post-bifurcation regimes; in fact, simple structures are modeled with imperfections included so that potential bifurcation points (such as B in Fig. 2.2a) are converted into maximum load points such as E. The buckling problem loses its special qualities as illuminated so skillfully in the asymptotic treatments and becomes just another nonlinear analysis, requiring perhaps special physical insight on the part of

the computer program user because of potential numerical traps such as spurious or real bifurcation points and ill-conditioning due to maximum load points or possibly outrageous shapes of some of the finite elements in the model.

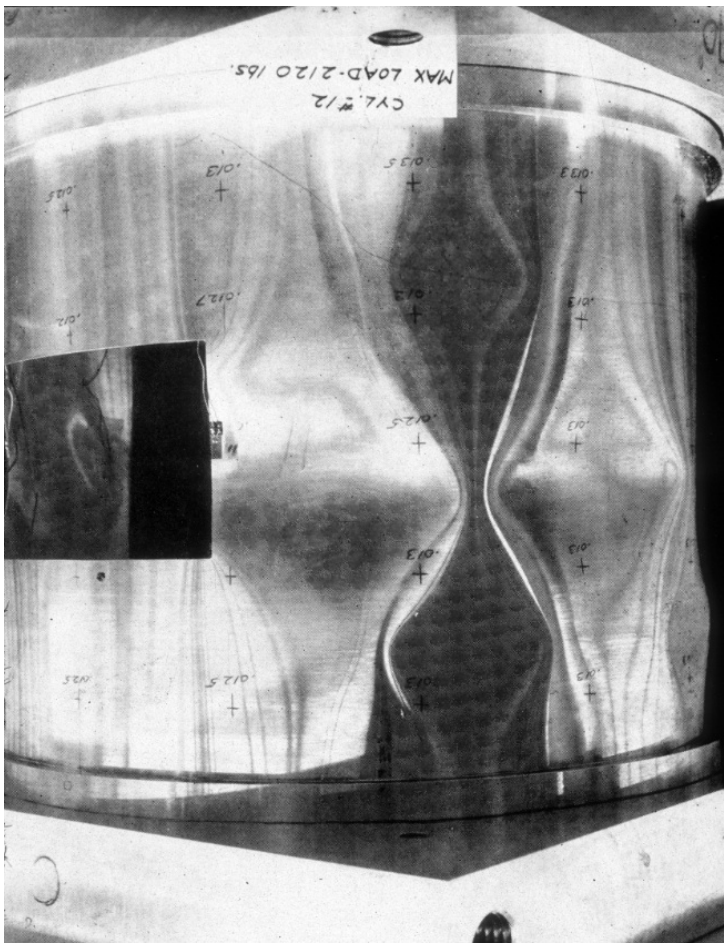

Buckling and collapse of an axially compressed, thin cylindrical shell under uniform end shortening. A general-purpose nonlinear finite element computer program such as STAGS is used for the prediction of the highly behavior of this non-axisymmetric shell. (Photograph by Bo O. Almroth and colleagues at the Lockheed Missiles & Space Company, mid 1960's; This picture is in the file, pitfallsnasa.ppt.)

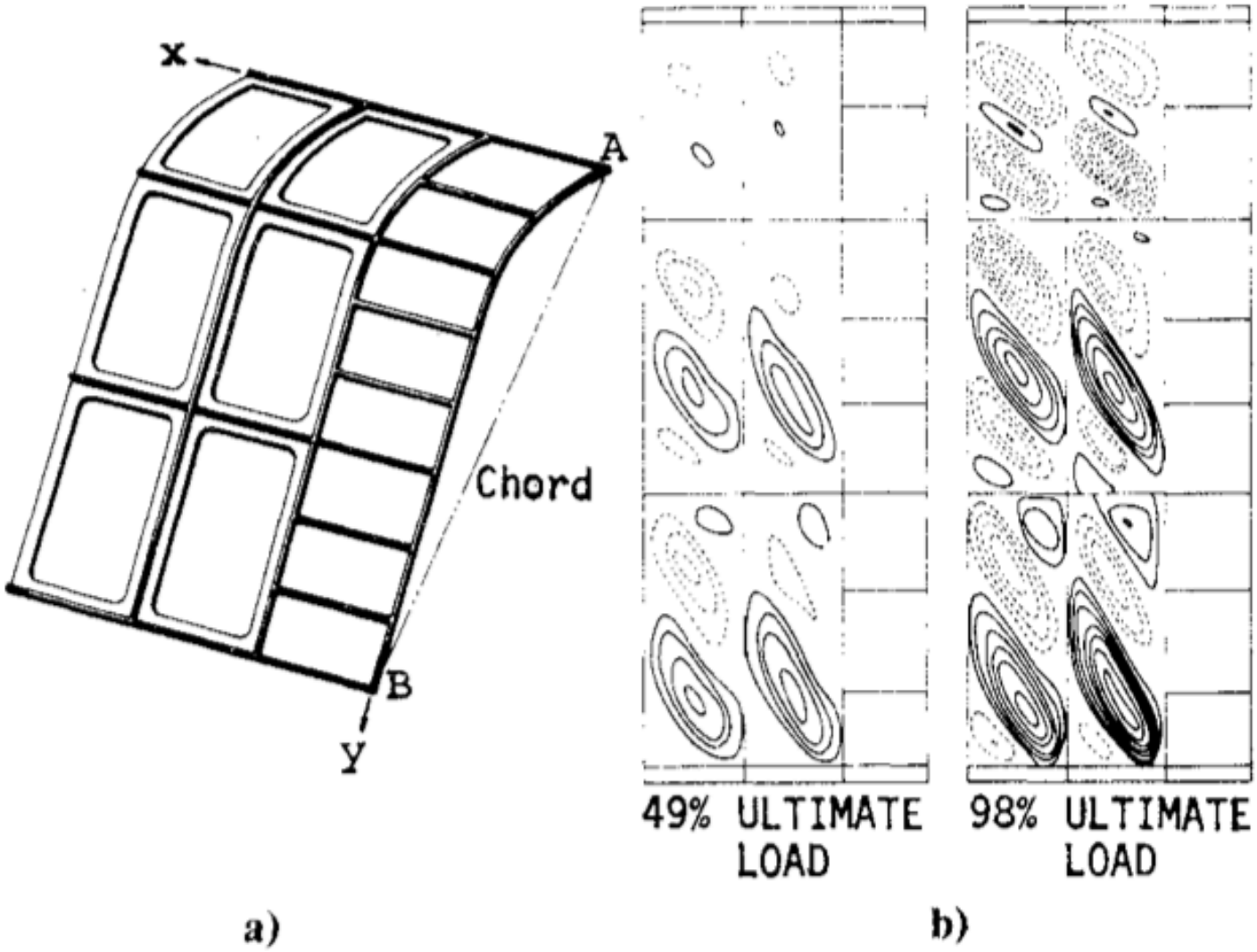

Fig. 6.7 Computer analysis of a complex shear panel (from Skogh and Stern [151]), a) Complex stiffened shear panel, b) Post-buckling behavior predicted with the STAGS computer program. (Fig. 6.7 in "Pitfalls" paper, AIAA Journal, Vol. 19, No. 9, 1981). [151] Skogh, J. and Stern, P. "Post-buckling Behavior of a Section Representative of the B-l Aft Intermediate Fuselage," AFFDL-TTR-73-63, May 1973.

PART 2

Presented at AIAA 48th Structures, Structural Dynamics and Materials Conference, AIAA-2007-2216, 2007

OPTIMIZATION OF AN AXIALLY COMPRESSED RING AND STRINGER STIFFENED CYLINDRICAL SHELLS WITH A GENERAL BUCKLING MODAL IMPERFECTION

David Bushnell, Fellow, AIAA, Retired, 775 Northampton Drive, Palo Alto, CA 94303, email: bush@sonic.net

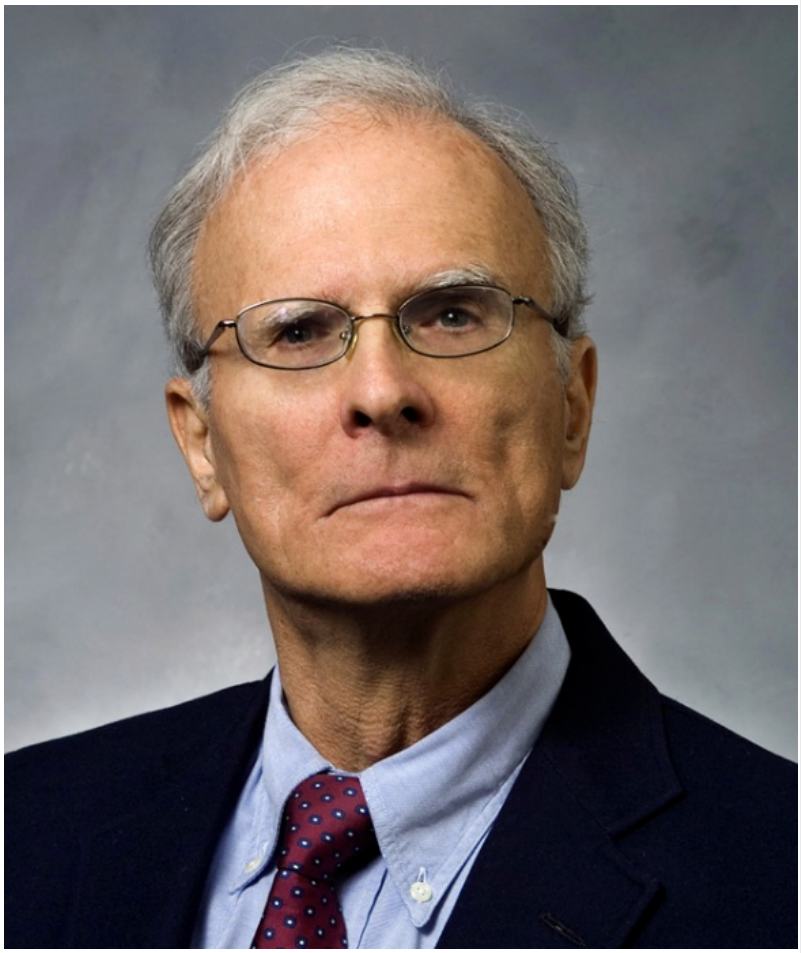

Dr. David Bushnell (2008)

It's hard to believe that this old coot is the same person as that depicted at the beginning of this file. David Bushnell worked at Lockheed Missiles & Space Company, which later became the Lockheed Martin Corporation, from 1961 to 1994, when he retired at age 55. In his retirement he continues to develop his computer programs, BIGBOSOR4, BOSOR5, PANDA2, and GENOPT. Most of his time, from 1994 to 2008, he spent on his continuing development of PANDA2, including the creation of the PANDA2 processors, PANEL, PANEL2, and PANEL3, that generate valid input files for BIGBOSOR4, and the PANDA2 processor, STAGSUNIT, that generates valid input files for the STAGS computer program, a general-purpose finite element code developed by Bo O. Almroth, Dr. Charles C. Rankin and others and currently being further developed by Dr. Rankin. From 2008 to the present Dr. Bushnell has worked primarily with GENOPT/ BIGBOSOR4, developing the capability to optimize complex shells of revolution and prismatic structures and validating the optimum designs by the application of STAGS. The pictures in this section are PANDA2-generated STAGS models of a ring and stringer stiffened, axially compressed cylindrical shell previously optimized by PANDA2.

ABSTRACT

PANDA2, a computer program for the minimum-weight design of elastic perfect and imperfect stiffened cylindrical panels and shells under multiple sets of combined loads, is used to obtain optimum designs of uniformly axially compressed elastic internal T-ring and external T-stringer stiffened cylindrical shells with initial imperfections in the form of the general buckling mode. The optimum designs generated by PANDA2 are verified by STAGS elastic and elastic-plastic finite element models produced automatically by a PANDA2 processor called STAGSUNIT. Predictions from STAGS agree well with those from PANDA2. Improvements to PANDA2 during the past year are summarized. Seven different optimum designs are obtained by PANDA2 under various conditions. The most significant condition is whether or not PANDA2 is permitted automatically to make the initial user-specified amplitude of the general buckling modal imperfection directly proportional to the axial half-wavelength of the critical general buckling mode. A survey is conducted over (m,n) space to determine whether or not the critical general buckling modal imperfection shape computed by PANDA2 with (m,n)critical (m=axial, n=circumferential) half-waves is the most harmful imperfection shape. It is found that indeed (m,n)critical is, for all practical purposes, the most harmful imperfection mode shape if PANDA2 is permitted automatically to make the general buckling modal imperfection amplitude directly proportional to the axial half-wavelength of the critical general buckling mode (inversely proportional to m). It is concluded that for axially compressed, stiffened, globally imperfect cylindrical shells the optimum designs obtained with the condition that PANDA2 is NOT allowed to change the initial user-specified imperfection amplitude are probably too heavy. One of the cases investigated demonstrates that the optimum design of a perfect shell obtained via the commonly used condition that a likely initial imperfection be replaced by an increase in the applied load by a factor equal to the inverse of a typical knockdown factor is too heavy. A new input index, ICONSV, is introduced into PANDA2 by means of which optimum designs of various degrees of conservativeness can be generated. Optimum designs are obtained with ICONSV = -1, 0, and +1, which represent increasing degrees of conservativeness in the PANDA2 model. It is concluded that, when obtaining optimum designs with PANDA2, it is best to allow PANDA2 to enter its branch in which local post-buckling behavior is determined, thereby avoiding the generation

of designs that may be unsafe because of excessive local bending stresses in the panel skin and stiffener parts. In most cases both nonlinear static and nonlinear dynamic analyses are required in order to obtain collapse loads with STAGS. A table is included that demonstrates how to use STAGS to evaluate an optimum design obtained by PANDA2. In most cases the elastic STAGS models predict collapse in one of the ring bays nearest an end of the cylindrical shell. With the effect of elastic-plastic material behavior included in the STAGS models, collapse most often occurs in an interior ring bay where the finite element mesh is the most dense.

From Section 7 of the same AIAA Paper 2007-2216:

7.0 TWO MAJOR EFFECTS OF A GENERAL BUCKLING MODAL IMPERFECTION (For some of the tables referenced, see 2007.axialcomp.pdf)

Much of the following appears in Section 11.1 on p. 19 of [1K] (Reference [1K] and other PANDA2 and STAGS references are given below). It is repeated here because this section is especially important. It briefly describes the behavior of a stiffened cylindrical shell with a general buckling modal imperfection shape. This behavior plays a major role in the evolution of the design during optimization cycles in PANDA2. Here it is assumed that the shortest wavelength of the general buckling modal imperfection is greater than the greatest stiffener spacing, as holds in Figs. 1 and 2, for example (disregarding the component of stringer bending-torsional deformation displayed in the expanded insert in Fig. 1a).

A general buckling modal imperfection in a stiffened shell has two major effects:

1. The imperfect stiffened panel or shell bends as soon as any loading is applied. This pre-buckling bending causes significant redistribution of stresses between the panel skin and the various stiffener parts, thus affecting significantly many local and inter-ring buckling and stress constraints (margins).

2. The "effective" circumferential curvature of an imperfect cylindrical panel or shell depends on the amplitude of the initial imperfection, on the circumferential wavelength of the critical buckling mode of the perfect and of the imperfect shell, and on the amount that the initial imperfection grows as the loading increases from

zero to the design load. The "effective" circumferential radius of curvature of the imperfect and loaded cylindrical shell is larger than its nominal radius of curvature because the larger "effective" radius corresponds to the maximum local radius of the cylindrical shell with a typical inward circumferential lobe of the initial and subsequently load-amplified buckling modal imperfection. In PANDA2 this larger local "effective" radius of curvature is assumed to be the governing UNIFORM radius in the buckling equations pertaining to the imperfect shell. For the purpose of computing the general buckling load, the imperfect shell is replaced by a new perfect cylindrical shell with the larger "effective" circumferential radius. By means of this device a complicated nonlinear collapse analysis is converted into a simple approximate bifurcation buckling problem - a linear eigenvalue problem. For each type of buckling modal imperfection (general, inter-ring, local [1E]) PANDA2 computes a "knockdown" factor based on the ratio:

(buckling load factor: panel with its "effective" circumferential radius)/
(buckling load factor: panel with its nominal circumferential radius) (7.1)

Figures 1a,b,c show a STAGS model of a typical general buckling modal imperfection shape (amplitude exaggerated) for an optimized "compound" model [1K] of an axially compressed cylindrical shell with external stringers and internal rings (Case 4 in Table 4 in this paper). In this compound model a 45-degree sector has both external stringers and internal rings modeled as flexible branched shell units. A 315-degree sector, the remainder of the cylindrical shell, has smeared stringers and internal rings modeled as flexible branched shell units. Figure 2 shows the deformed state of the imperfect compound model as loaded by the design load, N_X = -3000 lb/in axial compression (STAGS load factor PA is close to 1.0). One observes three characteristics:

1. The stresses in the imperfect axially compressed shell have been redistributed as the globally imperfect shell bends under the applied axial compression. The maximum effective (von Mises) stress in this case, sbar(max) = 66.87 ksi, occurs in the outstanding stringer flanges where the pre-buckling deformation pattern of the imperfect shell has a maximum inward lobe.

2. The typical maximum "effective" circumferential radius also occurs where the

deformation pattern has a maximum inward lobe. This larger-than-nominal circumferential radius is highlighted most clearly by the in-plane circumferential deformation of the interior ring located one ring spacing in from the right-hand curved edge of the STAGS model shown in Fig. 2. See the right-most expanded insert in Fig. 2.

3. There is an important phenomenon that occurs when **imperfect** cylindrical shells are optimized. This phenomenon has been described in previous papers [1K]. It occurs in the case of a stiffened cylindrical shell with an imperfection in the form of the critical general buckling mode of the perfect shell. The optimum design of an **imperfect** stiffened cylindrical shell has a general buckling load factor that is usually considerably higher than load factors that correspond to various kinds of local and "semi-local" buckling, such as local buckling of the panel skin and stiffener segments, rolling of the stiffeners, and inter-ring buckling. The general buckling margin of such a shell is usually not critical (near zero). In contrast, when a **perfect** stiffened cylindrical shell is optimized the general buckling load factor is usually very close to at least one local buckling load factor and is usually lower than many other local and "semi-local" buckling load factors. The general buckling margin of an optimized **perfect** shell is usually critical (near zero).

The cases explored in this paper exhibit this characteristic. Take, for example, the optimum designs called Case 1 and Case 2 in Table 4. In Case 1 a **perfect** shell is optimized. The margins for the Case 1 optimum design are listed in Table 10. (See Table 10 in panda2.papers/2007.axialcomp.pdf) Several of the margins for local and "semi-local" buckling are essentially equal to or greater than that for general buckling, and the general buckling margin is near zero (critical). In Case 2 a shell with a general buckling modal imperfection is optimized. The margins for the **imperfect** optimized shell are listed in Table 6, and those for the same optimum configuration but with the amplitude of the general buckling modal imperfection set equal to zero are listed in Table 7. In both Tables 6 and 7 of the paper, panda2.papers/2007.axialcomp.pdf, the margin for general buckling of the optimized **imperfect** shell is considerably higher than many of the margins corresponding to local and "semi-local" buckling. The general buckling margin of the optimized imperfect shell is well above zero (not critical).

Why does this happen? The general buckling margin of optimized IMPERFECT stiffened shells is forced higher during optimization cycles because PRE-BUCKLING BENDING OF THE IMPERFECT SHELL increases with applied load approximately hyperbolically as the applied load approaches the general buckling load of the imperfect shell [1E]. If the general buckling load of the optimized imperfect shell were close to the design load, that is, if the general buckling margin were near zero (almost critical), there would be so much pre-buckling bending near the design load that LOCAL STRESS AND BUCKLING MARGINS FOR THE STIFFENER PARTS AND FOR THE PANEL SKIN WOULD BECOME NEGATIVE BECAUSE THESE PARTS OF THE STRUCTURE WOULD BECOME HIGHLY STRESSED.

A table and several figures from the 2007 AIAA Paper 2007-2216, April, 2007 follow. (See panda2.papers/2007.axialcomp.pdf for the complete paper.)

Table 4 Optimum designs from PANDA2 suitable for analysis by STAGS (dimensions in inches)

.	**Case 1** Perfect, no Koiter, ICONSV=1	**Case 2** Imperfect, no Koiter, yes change imperfection amplitude, ICONSV=-1	**Case 3** Imperfect, no Koiter, yes change imperfection amplitude, ICONSV=0	**Case 4** Imperfect, no Koiter, yes change imperfection amplitude, ICONSV=1	**Case 5** Imperfect, yes Koiter, yes change imperfection amplitude, ICONSV=1	**Case 6** As if perfect, no Koiter, Nx=-6000, sbar=120 ksi ICONSV=1	**Case 7** Imperfect, no Koiter, no change in imperfection amplitude, ICONSV=1
Variable Name	Optimum Design	Optimum Design	Optimum Design	Optimum Design	Optimum Design	Optimum Design	Optimum Design
B(STR)	0.75519	0.93500	0.93500	0.98170	0.93500	0.93500	1.5708
B2(STR)	0.075519	0.093500	0.093500	0.0981710	0.093500	0.093500	0.15708
H(STR)	0.39795	0.57079	0.58395	0.63651	0.55261	0.55330	0.92254
W(STR)	0.35593	0.38639	0.36056	0.39946	0.29593	0.36761	0.64833
T(1)(SKN)	0.030240	0.033988	0.033795	0.034878	0.039964	0.044110	0.048160
T(2)(STR)	0.019897	0.028540	0.029197	0.031826	0.027631	0.033536	0.046127
T(3)(STR)	0.022209	0.026779	0.029411	0.022835	0.032576	0.024673	0.033702
B(RNG)	6.25	9.3750	8.3333	8.3333	9.3750	8.3333	15.000
B2(RNG)	0.0	0.0	0.0	0.0	0.0	0.0	0.0
H(RNG)	0.52160	0.79425	0.75877	0.79978	0.77659	0.92137	0.86341

W(RNG)	0.17891	0.10000	0.12313	0.24075	0.31922	0.35255	1.0804
T(4)(RNG)	0.026080	0.039713	0.037939	0.040078	0.038830	0.046069	0.043170
T(5)(RNG)	0.021847	0.097842	0.086763	0.029339	0.037873	0.017627	0.054020
WEIGHT	**31.81 lb**	**39.40 lb**	**40.12 lb**	**40.94 lb**	**41.89 lb**	**46.83 lb**	**56.28 lb**
Critical margins from PANDA2, Table 5	**1, 6a,b, 23a,b, 26, 44, 55, 56, 57, see Table 10**	**1, 3, 6a,c,e, 10, 23a, 26, 47, 55, 56, 57, see Table 6.**	**1, 3, 6a,c,e, 10, 23a, 26, 47, 55, 56, 57**	**1, 3, 6a,c,e, 10, 23a,e, 25, 26, 44, 47, 55, 56, 57**	**1, 3, 6a,d, 10, 11, 23a, 44, 47, 55, 56, 57**	**1, 3, 6a,c,e, 10, 11, 23a, 25, 26, 44, 47, 55, 56, 57, 58**	**1, 3, 6a,c,e, 10, 11, 23e, 25, 26, 44, 46, 55, 56, 57, 58**
Almost critical margins from STAGS and mode of elastic collapse	**1, 6a, 44, Collapse was not computed**	**1, 6a, 47, Stringer sidesway and first bay collapse at PA=1.04**	**1, 6a, 47, Stringer sidesway and first bay collapse at PA= 1.05**	**1, 6a, 47, Stringer sidesway and first bay collapse at PA=1.08**	**1, 6a, 47, Stringer sidesway and first bay collapse at PA=1.13**	**1, 6a, 11, 44, 47, Axisym-metric edge collapse at PA=0.970; rv(edge)=0 on 2 curved edges.**	**1, 6a, 11, 47, Stringer sidesway, first,middle and last bay collapse at PA= 1.22(–) PA= 1.15(+)**
Tables & Figures pertaining to the case	**Table 10, Figs. 3, 33-41**	**Figs. 8–32**		**Figs. 1a-c, 2, 4-7, 42-65**	**Table11, Figs. 66-71**	**Figs. 72-74**	**Figs. 75-80**
Comments	**This shell is not practi-cal because no one can fabricate a perfect structure.**	**With this option you MUST check the results via a general-purpose code such as STAGS.**	**With this option you are strongly URGED to check result with use of a general-purpose program.**	**This option may lead to shells with local skin & stringer bending & therefore possibly excessive stresses.**	**This is the best option if you do not plan to check PANDA2 designs. Even so, you SHOULD check them.**	**This widely used option generates a heavy shell. PANDA2 cannot predict axi-symmetric collapse.**	**This option is too con-servative, in my opinion. The imperf-ection can probably be detected easily.**

For a detailed explanation of the column headings in Table 4 see the full-length paper, panda2.papers/2007.axialcomp.pdf or the file, panda2.abstracts/2007.axialcomptable4.pdf.

PANDA2 and STAGS references:

[1] Bushnell, D., et al (**A**) "PANDA2 - Program for minimum weight design of stiffened, composite, locally buckled panels", Computers and Structures, Vol. 25 (1987) pp. 469-605. See also: (**B**) "Theoretical basis of the PANDA computer program for preliminary design of stiffened panels under combined in-plane loads", Computers and Structures, v. 27, No. 4, pp 541-563, 1987; (**C**) "Optimization of composite, stiffened, imperfect panels under combined loads for service in the post-buckling regime", Computer Methods in Applied Mechanics and Engineering, Vol. 103, pp 43-114, 1993; (**D**) "Recent enhancements to PANDA2" 37th AIAA Structures, Dynamics, and Materials (SDM) Conference, April 1996; (**E**) "Approximate method for the optimum design of ring and stringer stiffened cylindrical panels and shells with local, inter-ring, and general buckling modal imperfections", Computers and Structures, Vol. 59, No. 3, 489-527, 1996, with W. D. Bushnell; (**F**) "Optimum design via PANDA2 of composite sandwich panels with honeycomb or foam cores", AIAA Paper 97-1142, AIAA 38th SDM Conference, April 1997; (**G**) "Additional buckling solutions in PANDA2", AIAA 40th SDM Conference, p 302-345, April 1999, with H. Jiang and N. F. Knight, Jr.; (**H**) "Minimum-weight design of a stiffened panel via PANDA2 and evaluation of the optimized panel via STAGS", Computers and Structures, Vol. 50, 569-602 (1994); (**I**) "Optimization of perfect and imperfect ring and stringer stiffened cylindrical shells with PANDA2 and evaluation of the optimum designs with STAGS", AIAA Paper 2002-1408, pp 1562-1613, Proceedings of the 43rd AIAA SDM Meeting, April, 2002, with C. Rankin; (**J**) “Optimum design of stiffened panels with substiffeners, AIAA Paper 2005-1932, AIAA 46th SDM Conference, April 2005, with C. Rankin; (**K**) “Difficulties in optimization of imperfect stiffened cylindrical shells, AIAA Paper 2006-1943, AIAA 47th SDM Conference, April 2006, with C. Rankin; (**L**).../panda2/doc/panda2.news, a continually updated file distributed with PANDA2 that contains a log of all significant modifications to PANDA2 from 1987 on; (**M**) “Optimization of Stiffened Panels in Which Mode Jumping is Accounted For,” AIAA Paper No. AIAA 97-1141, AIAA 38th SDM Conference, April 1997, with C. Rankin and E. Riks.; (**N**) “Global Optimum Design Of Externally Pressurized Isogrid Stiffened Cylindrical Shells With Added T-Rings,” International Journal of Non-Linear Mechanics Vol. 37, pp. 801–831, 2002; (**O**) “Optimization of an axially compressed ring and stringer stiffened cylindrical shell with a general buckling modal imperfection,” AIAA Paper No. AIAA 2007-

2216, AIAA 48th SDM Conference, April, 2007; (**P**) "Optimization of panels with riveted Z-shaped stiffeners via PANDA2", in *Advances in the Mechanics of Plates and Shells,* Durban, D, Givoli, D., and Simmonds, J.G., Eds, Kluwer Academic Publishers, pp 79-102, 2001; (**Q**) "Global Optimum Design Of Externally Pressurized Isogrid Stiffened Cylindrical Shells With Added T-Rings," International Journal of Non-Linear Mechanics Vol. 37, pp. 801–831, 2002

[18] Almroth, B. O. and Brogan, F. A., "The STAGS computer code", NASA CR-2950, NASA Langley Research Center, Hampton, VA, 1978.

[19] STAGS Brochure (2002) available online by request: crankin@rhombuscgi.com (pdf format).

[20] (**A**) Rankin, C.C., Stehlin, P., and Brogan, F.A., "Enhancements to the STAGS computer code", NASA CR-4000, NASA Langley Research center, Hampton, VA, 1986. See also: (**B**) Rankin, C.C, "Application of Linear Finite Elements to Finite Strain Using Corotation." AIAA Paper AIAA-2006-1751, 47th AIAA Structures, Structural Dynamics and Materials Conference, May 2006; (**C**) Rankin, C.C., Brogan, F.A., Loden, W.A., Cabiness, H.D., "STAGS User Manual – Version 5.0," Rhombus Consultants Group, Inc., Palo Alto, CA, Revised January 2005 (on-line). Previously Report No. LMSC P032594, Lockheed Martin Missiles and Space Company, Palo Alto, CA, June 1998; (**D**) Rankin, C.C., "The use of shell elements for the analysis of large strain response, AIAA Paper 2007-2384, 48th AIAA Structures, Structural Dynamics and Materials Conference, Hawaii, April 2007.

[21] Riks, E., Rankin C. C., Brogan F. A., "On the solution of mode jumping phenomena in thin walled shell structures", First ASCE/ASM/SES Mechanics Conference, Charlottesville, VA, June 6-9, 1993, in: Computer Methods in Applied Mechanics and Engineering, Vol. 136, 1996.

SOME ADVICE:

The following figure captions cite figures and tables that are not included here. Please see the complete paper, panda2.papers/2007axialcomp.pdf, for more details.

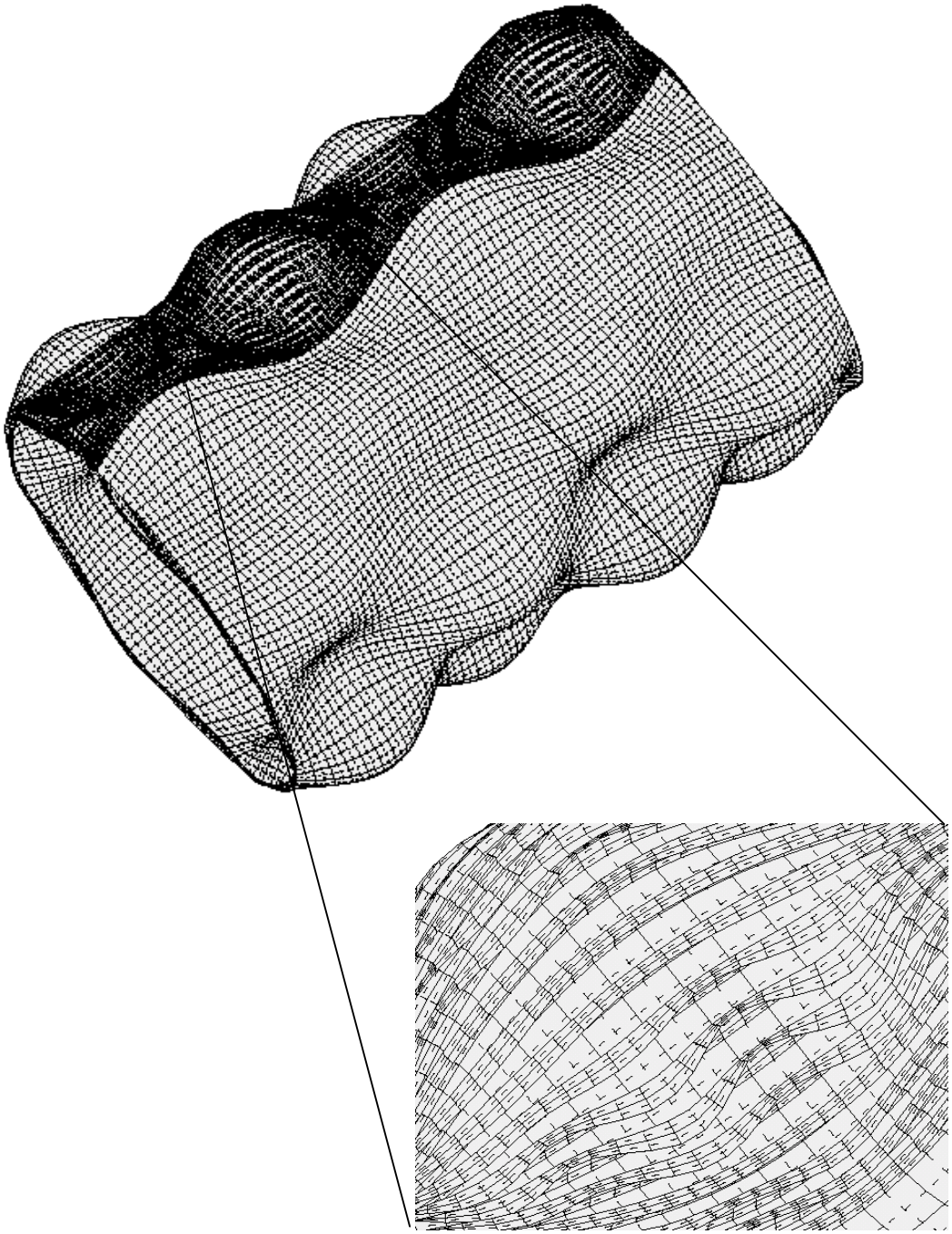

Case 4 in Table 4 no Koiter, yes change imperfection, ICONSV=1; compare with Fig.49. STAGS Mode 395 = lowest general buckling mode, load factor, pcr=2.0308; BIGBOSOR4 predicts 2.0008 (m,n)=(4 axial halfwaves, 6 circumferential full waves); PANDA2 predicts 2.07 before knockdowns for smearing stringers, for smearing rings, and for transverse shear deformation (t.s.d). PANDA2 predicts 1.774 after application of these three knockdowns. Note from the expanded insert that the general buckling mode includes a significant component of bending-torsion buckling of the stringers.

FIG.1a Linear general buckling mode from a "compound" STAGS model. The nodal mesh density is not sufficiently refined to capture local skin/stringer bending and buckling of the type shown in Fig. 23a. Compare Fig. 1a with Fig. 49.

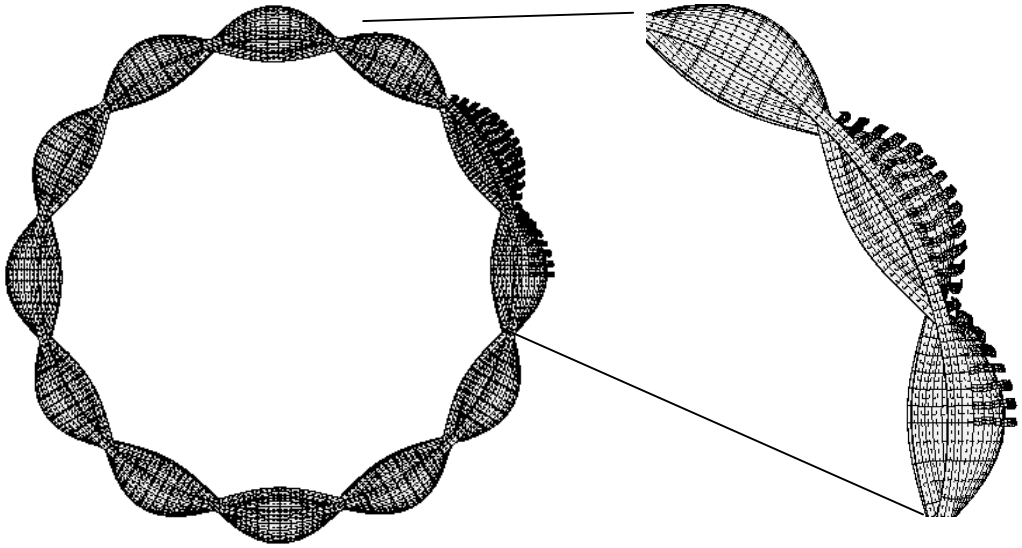

Case 4, Table 4: no Koiter, yes change imperfection, ICONSV=1. STAGS Mode 395 = general buckling; load factor, pcr=2.0308; first of a pair of modes. The region with stringers modeled as shell units spans 45 degrees of circumference.
FIG. 1b End view of the same linear buckling mode as that shown in the previous figure

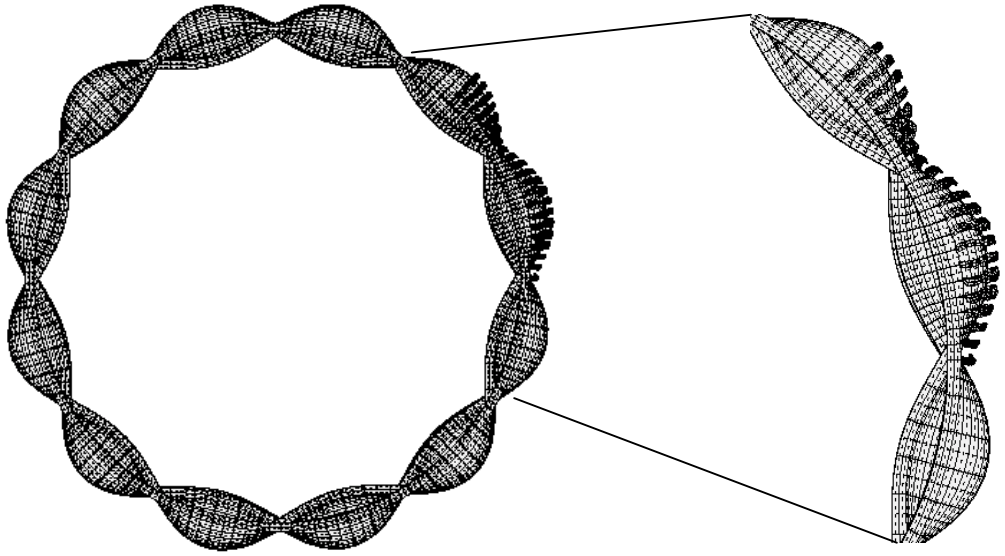

Case 4, Table 4: no Koiter, yes change imperfection, ICONSV=1. Compare with Fig. 1b. With a complete (360-deg) cylindrical shell the modes always occur in pairs. STAGS Mode 396, buckling load factor, pcr=2.0309; second of a pair of modes.
FIG. 1c End view of the next buckling mode to that shown in the previous figure.

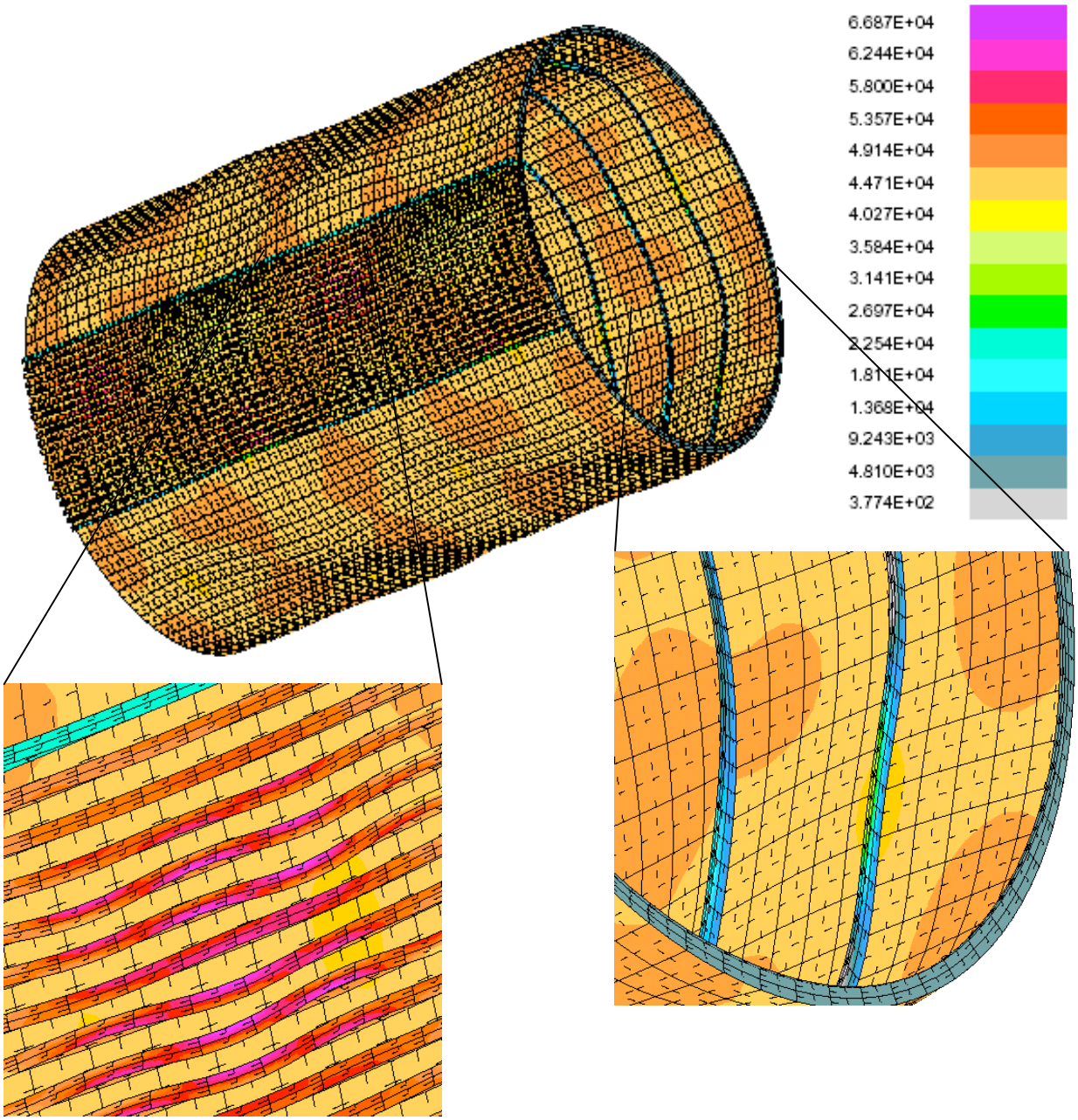

Case 4, Table 4: no Koiter, yes change imperfection, ICONSV=1; also see Figs. 61-63. Nonlinear equilibrium state from STAGS at the load factor, PA=1.00516. The imperfect shell has two initial buckling modal imperfection shapes: Fig. 1a with amplitude, Wimp1=+0.0625 and Fig. 61 with amplitude, Wimp2= -0.0005 inch. Pre-buckling bending of the imperfect shell causes redistribution of stresses among the shell skin and the stiffener segments. Also, pre-buckling bending gives rise to "flattened" regions with an "effective" circumferential radius of curvature that causes early general buckling. (See the right-most expanded insert).
FIG. 2 STAGS prediction of outer fiber effective stress (psi) at axial load, Nx= -3000 x 1.00516 lb/in.

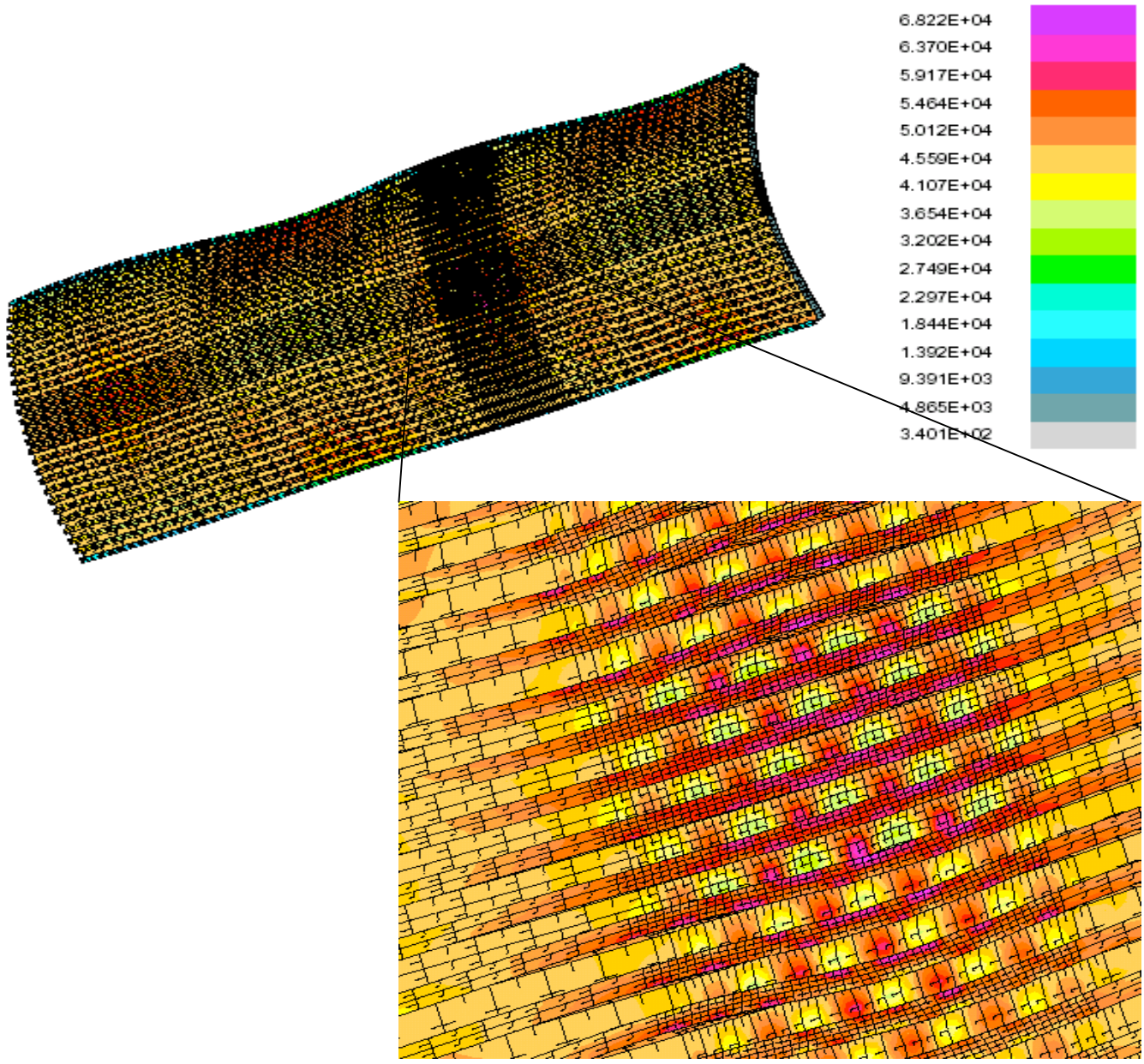

Case 4, Table 4 no Koiter, yes change imperfection, ICONSV=1; Compare with Fig.2. Deformed state during a nonlinear dynamic STAGS run at the design load, PA=1.0, Time = 0.00255 seconds (Fig.52). Notice local bending in the panel skin. The imperfect shell has only a general buckling modal imperfection shape (that shown in Fig. 49) with amplitude, Wimp1 = -0.0625 inches. This is a 60-degree STAGS model of the same configuration (Case4) as that shown in Figs. 1 and 2 with symmetry conditions applied along the two straight edges. The agreement of predictions from the 360-degree compound model and the 60-degree model justifies use of the 60-degree model.
FIG. 7 STAGS prediction of outer fiber effective stress (psi) at the design load, Nx = -3000 lb/in.

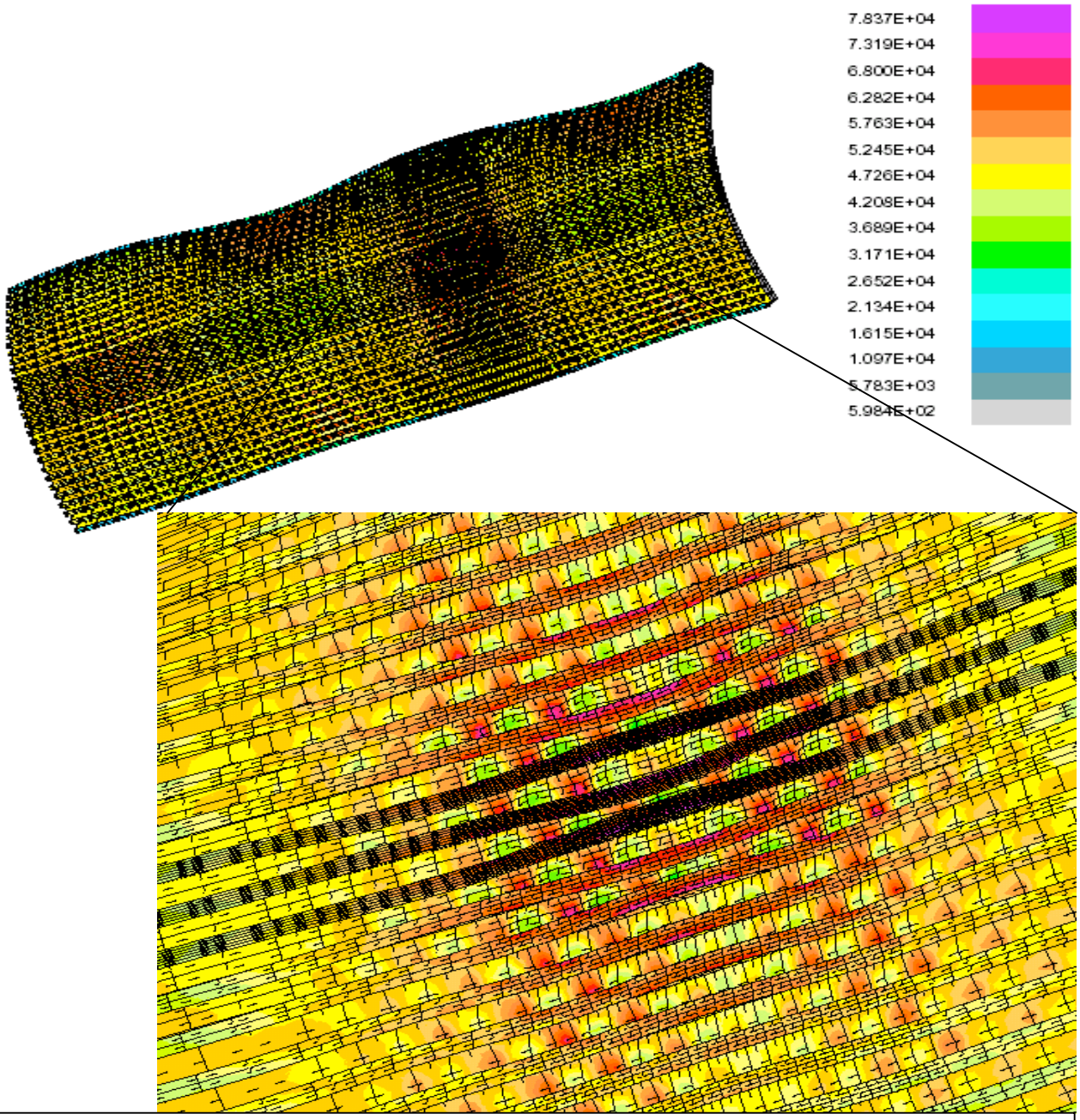

Case 2, Table 4: no Koiter, yes change imperfection, ICONSV=-1. See Part 8 of Table 9. Imperfect shell with same 3 imperfections as identified in the previous figure. Deformed state predicted by STAGS at the highest load factor reached in the nonlinear static run, PA = 1.02487. **FIG. 29 Outer fiber effective stress (psi) at axial load Nx = -3000 x 1.02487 lb/in. Compare with previous figure. Notice sidesway of the three central stringers in the region with the highest mesh density. (The three central stringers are darker than the others because they have greater nodal point density over their cross sections)**.

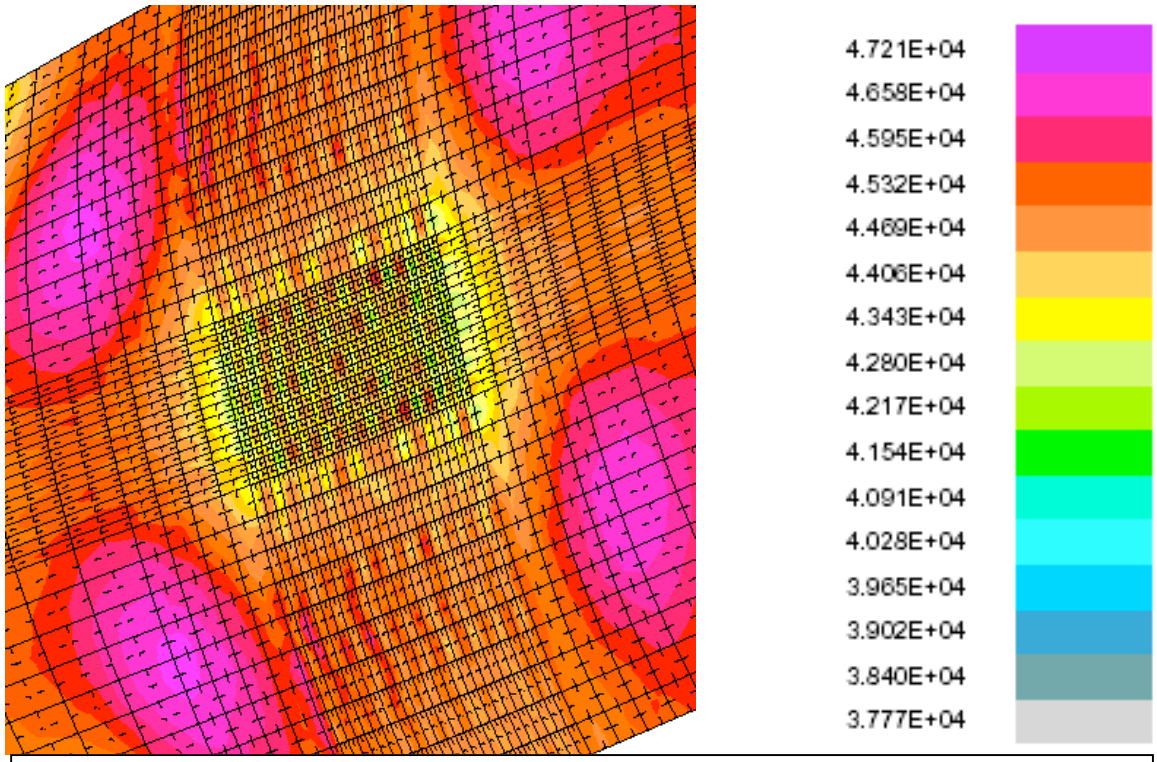

Case 4, Table 4: no Koiter, yes change imperfection, ICONSV = 1. Compare with Fig. 50. Imperfection shape shown in Fig. 49, amplitude, Wimp=-0.0625 in. Deformed state in the panel skin (shell unit no. 1) from STAGS at the highest load factor reached in the nonlinear static run, PA=0.98.
FIG. 51 STAGS prediction of outer fiber effective stress (psi) in the panel SKIN at axial load, Nx= -3000 x 0.98 lb/in.**i) in the panel SKIN at axial load, Nx= -3000 x 0.98 lb/in.**

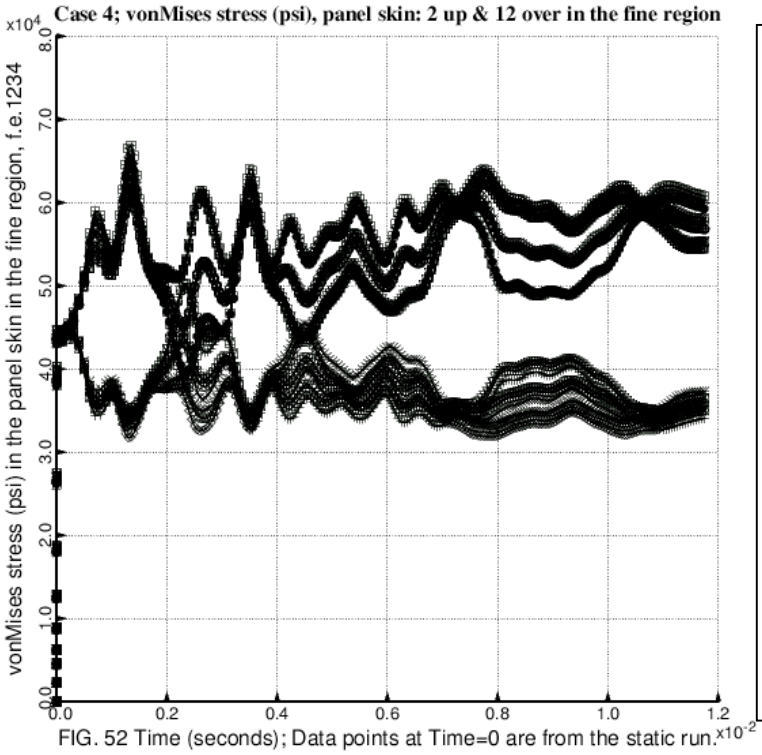

FIG. 52 Case 4 in Table 4: The large increase in effective (vonMises) stress in the panel skin during the dynamic STAGS run in which the load factor is held constant at PA = 1.0 (the design load) is caused by local buckling of the type displayed in Figs. 4 and 48. This local buckling at PA = 1.0, occurring for an optimum design configuration derived with use of the "no Koiter" option, is the reason that in Table 4 the recommended option is to use "yes Koiter". (See Case 5).

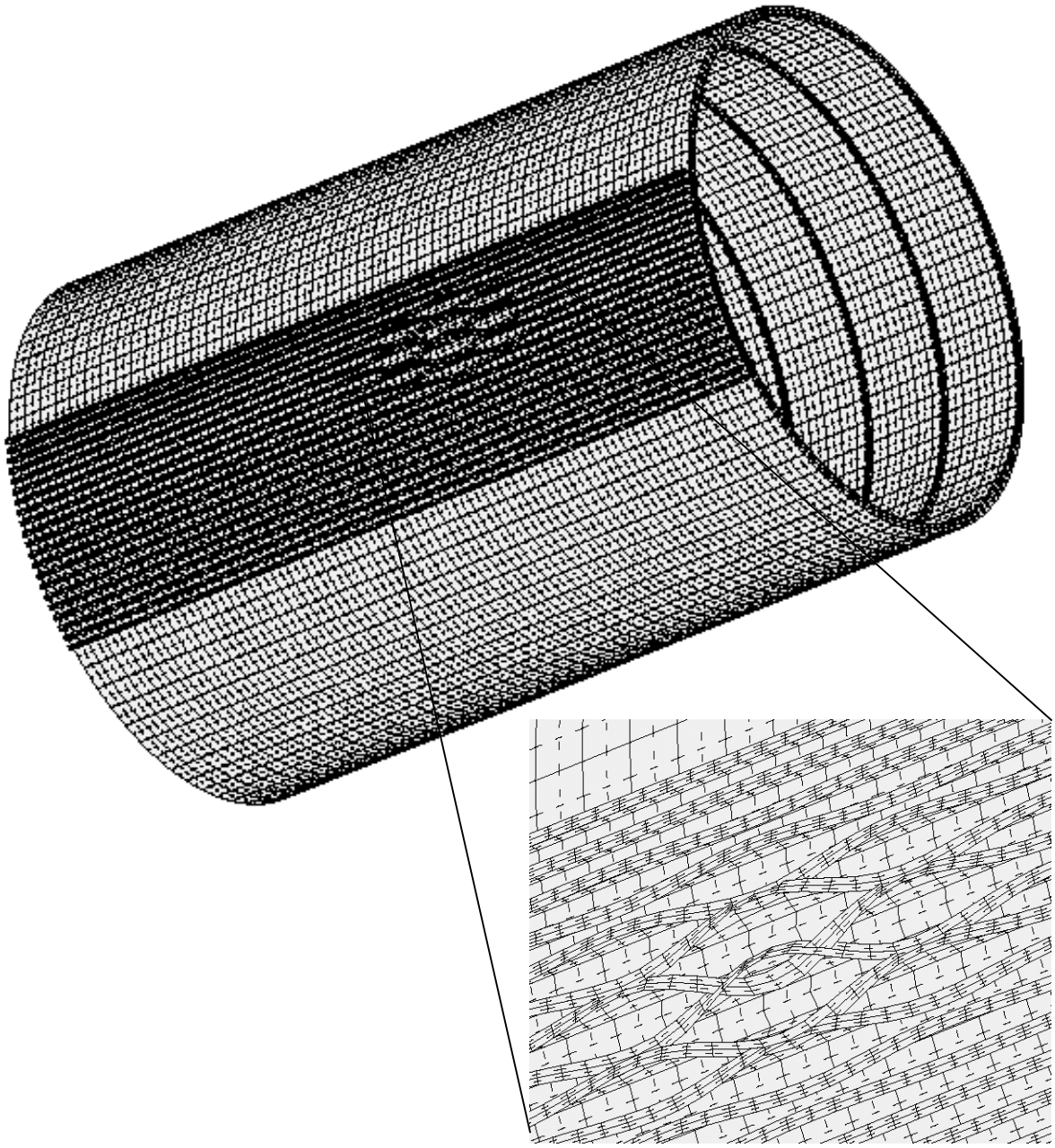

Case 4, Table 4: no Koiter, yes change imperfection, ICONSV = 1. STAGS nonlinear buckling mode at load factor, PA = 1.07084. There is one imperfection shape, shown in Figs. 1a,b, with amplitude, Wimp1=+0.0625 inch. The nonlinear buckling load factor from STAGS, pcr=1.1386; PANDA2 predicts 1.0097 for the bending-torsion buckling mode of the imperfect shell as loaded by the design load, Nx= -3000 lb/in.

FIG. 61 NONLINEAR bending-torsion buckling mode from STAGS. This mode is used as a second imperfection shape with amplitude, Wimp2 = -0.0005 inch in a subsequent nonlinear STAGS run.

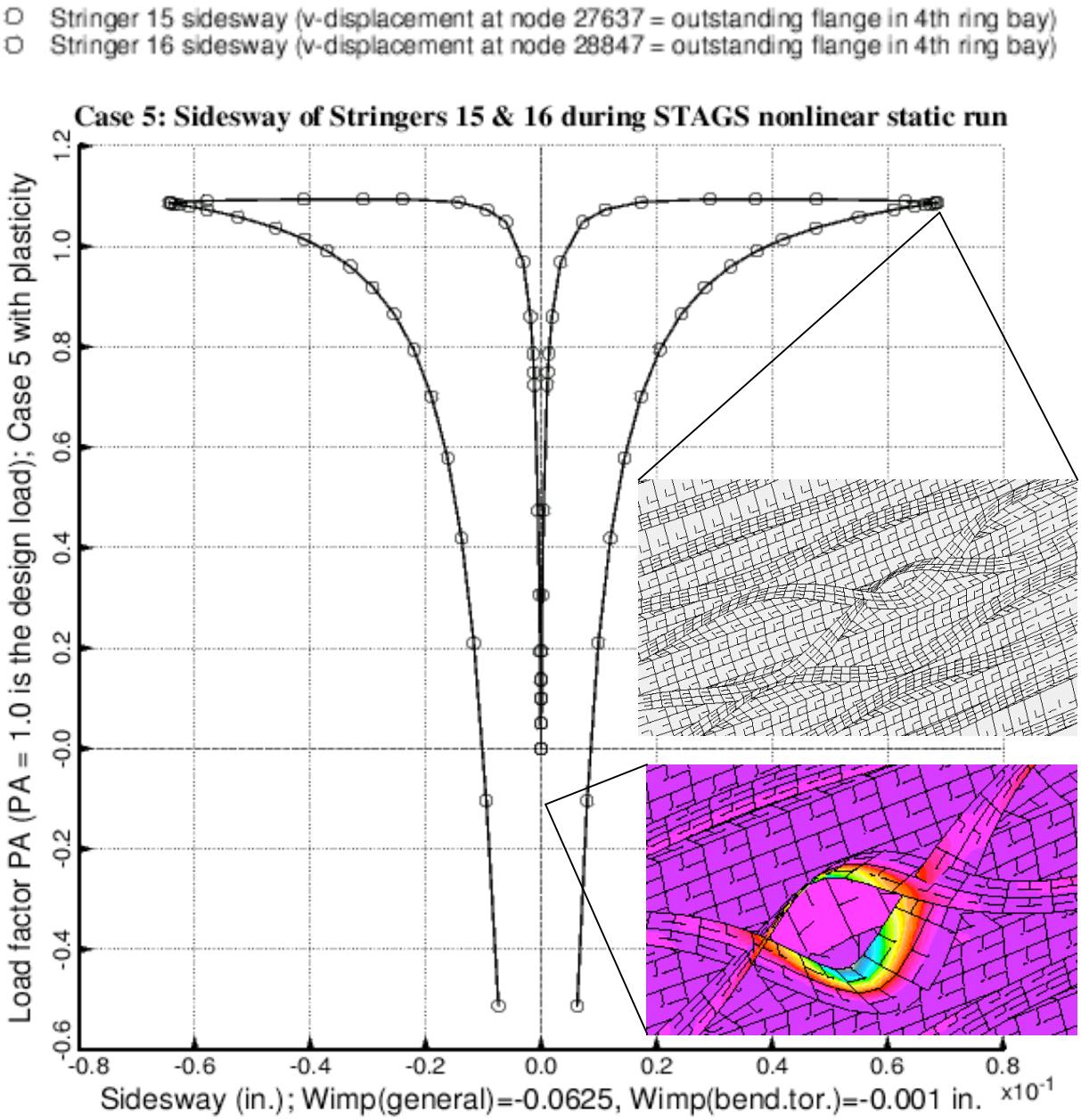

FIG. 93 STAGS model of Case 5, Table 4 with **plasticity included**. Nonlinear static elastic-plastic sidesway of Stringers 15 & 16 (numbering from the bottom in Figs. 66 & 67) in Ring bays 3 & 4 (Fig. 66). Two imperfection shapes: **1**. general buckling modal imperfection shape similar to that in Fig. 66 with amplitude, Wimp1 = -0.0625 inch, and **2.** bending-torsion buckling shape similar to that shown in the lower expanded insert in Fig. 68 with amplitude, Wimp2 = -0.001 inch. In the bending-torsion imperfection shape in this elastic-plastic model there is no buckling modal deformation near the right-hand end of the shell. Compare with Figs. 69-71.

PART 3:
Some advice to colleagues relating to buckling of shells

David Bushnell

CHAPTER 1
HOW TO DETERMINE IF A STRUCTURE IS BUCKLING-SAFE
------- 22 October 2007 (modified, January 9, 2008: -----

Here is a message in which I describe what I feel is a generally valid procedure to determine whether or not a structure previously modeled with any general-purpose computer program for a stress analysis is buckling-safe.

The following letter, reproduced below, was written to my colleague, Frank. Frank had asked me what he should do to assure that a structure he was analyzing for one of the engineering divisions would not buckle. He already had a very detailed ABAQUS finite element model, and he had performed a stress analysis.

Now, I have never used ABAQUS and don't know what its capabilities are. However, despite this gross ignorance on my part, I wrote Frank the following message. In my opinion a procedure such as that described below should work in any context in which an engineer wants to determine if a structure is buckling-safe.

October 18, 2007

Dear Frank:

I've been thinking about your structural buckling problem while I lie abed very early in the morning. I have come up with the following suggestions.

First, let me introduce a few definitions applicable to a **linear** buckling formulation:

1. A linear buckling eigenvalue equation is:

$$[K1]\{q\} = \text{lambda}[K2]\{q\} \qquad (1)$$

in which [K1] is the stiffness matrix for the structure as loaded by “Load Set B”; [K2] = Load-geometric matrix for the structure as loaded by “Load Set A”; {q} = buckling eigenvector, that is, the buckling mode shape; lambda = buckling eigenvalue (buckling load factor). Example: suppose you want to find the buckling pressure of a cylindrical shell under uniform external pressure (“Load Set A”) and under uniform axial tension that has a “fixed” value, that is, axial tension that you know in advance and that is not to be multiplied by the eigenvalue, lambda (“Load Set B”).

2. “Load Set A” = loads from which [K2] is computed, that is, the loads corresponding to which you want to find a buckling load factor (eigenvalue). In the example “Load Set A” = uniform external pressure.

3. “Load Set B” = loads which affect [K1], that is, the loads that are “fixed” in the sense that they represent part of the structural system in the same way that stiffnesses and boundary conditions represent the structural system. In this example “Load Set B” = uniform axial tension.

The following suggestions are based on the assumption that all the loads are either in "Load Set A" (that is, all the loads are "eigenvalue" loads) or any loads that happen to be in "Load Set B" (that is, "non-eigenvalue" or “fixed” loads) are **stabilizing.** I'm assuming that there are no "fixed" pre-loads, such as fixed **destabilizing** thermal loads and/or fixed **destabilizing** pressure or other **destabilizing** "mechanical" loads. If it is hard to tell whether Load Set B loads are stabilizing or destabilizing, then do what you would do assuming that the loads in Load Set B are destabilizing. If there are significant destabilizing loads in Load Set B, then first perform a linear buckling analysis with all the loads in Load Set A set equal to zero and all the loads in Load Set B transferred to Load Set A. Check to see if this case yields any eigenvalues that are less than unity. If not (or if all eigenvalues less than unity are negative) then proceed as described below. If so, then the

structure will buckle under Load Set B acting by itself and it must therefore be redesigned (or there might be something wrong with your modeling or with your specification of Load Set B).

Assuming that there are no "Load Set B" problems, proceed as follows:

Item no.1. Run a **linear** buckling analysis at 1g acceleration. (NOTE: In Frank Weiler's particular structural problem the "Load Set A" loading was weight. This weight acted sort of like a nonuniform external pressure on a short cylindrical shell.) I expect you'll probably find a reasonably high (safe) buckling load factor (eigenvalue), but that might possibly not be so in your case (see **Item no. 3**).

Caution 1: Your analysis is for a PERFECT structure. The question always arises, what is the sensitivity of the buckling load factor to **initial imperfections**? This, of course, depends on the nature of the structure and the loading. If you find that the pre-buckling state in the area where buckles first occur indicates relatively uniform axial compression in a thin cylindrical shell, then you probably should apply a knockdown factor of at least 2.0. It is to be hoped that the linear/nonlinear buckling analyses will yield buckling load factors that are high enough that you don't have to worry about initial imperfections.

Caution 2: I think yesterday you said that there are contact elements in your structure. Suppose you find that buckling occurs in a region where considerations of contact are important. A question arises: "How does ABAQUS model bifurcation buckling in a region where contact elements exist? For example, suppose you have a thin cylindrical shell (a "liner") encased in a relatively soft material, all under external pressure. During the buckling process the thin cylindrical shell is free to separate from the surrounding soft material where inward buckles develop, but pushes into this surrounding soft material where outward buckles develop. How does ABAQUS handle this? Perhaps a linear eigenvalue analysis is not sufficiently accurate.

Item No.2. Run a **nonlinear** buckling analysis at 1g acceleration. There probably won't be much difference from the linear result if the linear result yields a reasonably high buckling load factor. If the nonlinear buckling load factor agrees fairly well with the linear (which is the case in most designs), and if the buckling load factor for a loading of 1g acceleration is reasonably high (that is the structure is safe from buckling), then you are done. If the nonlinear buckling load factor disagrees with the linear buckling load factor, is **higher** than the linear buckling load factor, and the linear buckling load factor is reasonably high, you are done. A nonlinear buckling load that is **higher** than the linear buckling load indicates that either the destabilizing (negative) pre-buckling internal loading of the structure increases more gradually (more slowly) with increasing load factor than does that corresponding to the linear theory, or the pre-buckling deformation is of such a nature as to stabilize the structure, or both. If the nonlinear buckling analysis yields a significantly **lower** buckling load factor than does the linear buckling analysis, but the nonlinear buckling load factor is still rather high (indicating a buckling-safe structure), then you are done. A nonlinear buckling load that is **lower** than the linear buckling load indicates that either the destabilizing (negative) pre-buckling internal loading of the structure increases more steeply than does that corresponding to the linear theory, or the pre-buckling deformation is of such a nature as to destabilize the structure (such as pre-buckling flattening of a cylindrical shell in the region where it buckles), or both. It is possible (though unlikely) that even though the linear buckling load factor indicates a buckling-safe structure, the nonlinear buckling load factor does not. If that unlikely event holds, proceed as in **Item 3.** Otherwise, you are done.

Item No. 3. If the linear buckling analysis at 1g acceleration yields a buckling load factor that is unacceptably low (taking possible imperfection sensitivity and the effects of contact into account), then there are two possibilities:

a. It is possible (although unlikely) that a nonlinear buckling analysis will solve the problem for you. (Believe it or not, this actually happened in one case in my past!) The nonlinear buckling eigenvalue may be higher than the linear buckling eigenvalue by enough to render the structure buckling-safe. In that unlikely case you are done. (Although I'll bet you'd have a difficult time persuading the customer that the structure is buckling-safe under this circumstance!)

b. More likely, nonlinear effects are harmful, that is, they "soften" the structure, making it appear to be less stable than does the linear theory or nonlinear effects are not significant enough to change the verdict, "buckling-unsafe structure". In this most likely of findings under this item (**Item no. 3**) the best solution is first to redesign the structure before you attempt any more precise buckling analyses, such as nonlinear load stepping. If it is not feasible or possible to redesign the structure, and if you must obtain a more precise prediction of the structural behavior, I suggest you do the following:

i. Obtain one or more imperfection shapes from linear buckling theory. Use as imperfection shapes one or more linear buckling modes. Assign as amplitudes of these buckling modal imperfection shapes values that are in keeping with the engineering tolerances specified in your project.

ii. Perform nonlinear equilibrium analyses of the imperfect structure by load stepping. Be careful to use as imperfection amplitude(s) the proper algebraic sign(s), that is, the algebraic sign(s) that render the imperfection shape(s) which are most harmful. If you don't know what sign(s) to use, you just have to do at least two nonlinear analyses for each imperfection shape, one with positive and the other with negative sign of the amplitude of the initial imperfection(s).

iii. Look for nonlinear collapse or excessive stresses that occur during the nonlinear load steps.

I hope this is helpful, Frank!

Dave

CHAPTER 2
CONCERNING FACTORS OF SAFETY
---------- by David Bushnell, 25 August 2007:

Suppose you have two computer programs, Program A and Program B, that supposedly do the same thing: find the minimum-weight design of an elastic stiffened cylindrical shell.

Assume that Program A is based on the simplest possible model: membrane pre-buckling behavior (that is, uniform pre-buckling stress resultants, Nx, Ny, Nxy), smeared stiffeners (without any compensating knockdown factors to account for the inherent unconservativeness of a smeared-stringer and/or smeared-ring model), stiffener cross sections not permitted to deform, perfect shell (no buckling modal imperfections), and linear bifurcation buckling model (no nonlinear effects at all).

Assume that Program B accounts for some pre-buckling bending, has knockdown factors to compensate for the inherent unconservativeness of smearing stiffeners, discrete stiffeners that can deform locally, buckling modal imperfections, and a "quasi-linear" bifurcation bucking model that accounts for the nonlinear pre-buckling growth of the initial buckling modal imperfections with increasing applied load, Nx, Ny, Nxy, p.

If you use the same factors of safety and the same design load for both computer Program A and computer Program B, you will usually obtain a heavier optimum design with Program B than with Program A.

The purpose of this email message (sent to a colleague at the NASA Langley Research Center, Hampton, Virginia) is to emphasize that you have to give a lot of thought to what

factors of safety and what loading you want to use in order to obtain your optimum design.

What I like to do whenever I obtain an optimum design is the following:

1. Use for the **design load** combination the **ULTIMATE** load, that is, the load combination, Nx, Ny, Nxy, p, that the structure would have to survive in its most rigorous static test. (This applies to multiple load combinations that the structure would have to survive with each ultimate load combination applied separately).

2. In PANDA2 generally use factors of safety for buckling equal to 0.999. (In PANDA2 when you use 0.999 for a buckling factor of safety PANDA2 does **not** automatically change the factor of safety to 1.1 the way it does if you use a buckling factor of safety between 1.0 and 1.09999). If you wish to allow local buckling at a lower load than the design load, then you must use a factor of safety for local buckling that is less than 0.999, say, 0.7 for a small amount of local post-buckling or 0.1 for a large amount of local post-buckling, for examples. If you do **not** want to permit any local post-buckling but you still for some reason want local buckling to occur at a lower load than general buckling, then use a buckling load factor of safety for local buckling of 0.999 and a buckling load factor of safety for general buckling something like 1.3, for example. I think it's best always to optimize with use of the YES KOITER option in the *.OPT file. (See Case 5 and compare its optimum design with that for Case 4 in my most recent PANDA2 paper, AIAA Paper 2007-2216, April 2007). (2011 NOTE: See Table 4 from that paper listed in PART 2 above.)

Often (it seems to me) factors of safety are dictated from "on high"; the designer doesn't have a choice in the matter. This management policy is poor, in my opinion, because then computer programs that include the most sophisticated models lead to the heaviest designs. You just penalize yourself by including a very sophisticated model for maximum stress, for example, and then applying to the predictions from this sophisticated model the same "traditional" factor of safety

that you would have applied to the simplest "membrane" model. Might as well use the simplest "membrane" model if your management is unbending with regard to what factor of safety to use.

For example, if you include the effect of initial imperfections in your structural model you do not also want to include a factor of safety that in the past compensated for our lack of ability to predict many years ago the deleterious effects of initial imperfections on shell buckling.

PART 4:
Slide 41 of my "Pitfalls" lecture, followed by a discussion of it:

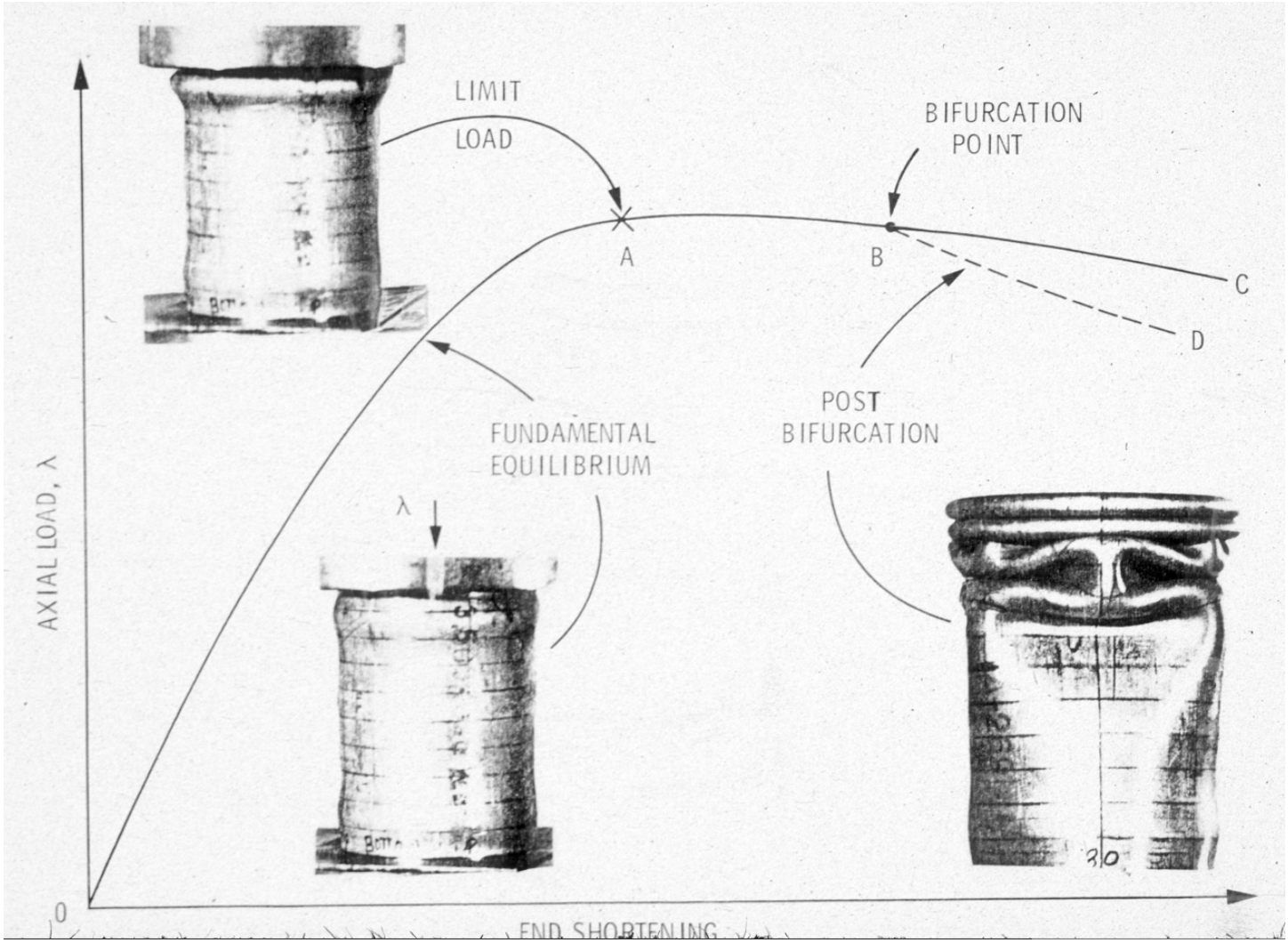

This is a very important slide, so please pay close attention! A rather thick aluminum cylindrical shell under uniform end shortening (axial compression). The primary equilibrium path (solid line, 0AC) corresponds to axisymmetric deformation, in which an elastic-plastic "elephant's foot" buckle develops, in this case, near the top end of the shell. In this particular case at a point, A, the maximum load-carrying capacity is reached. As end shortening is further increased, at another point, B, bifurcation of equilibrium states initiates. The dotted path, BD, corresponds to equilibrium states in which the total deformation consists of further axisymmetric deformation plus a rapidly growing component of non-axisymmetric deformation. The bifurcation point, B, can be determined from a series of nonlinear eigenvalue analyses in which the uniqueness of the equilibrium state on the primary (axisymmetric) equilibrium path is tested at successive points on this path. The

point on the primary path at which the stability determinant first equals zero (non-uniqueness of equilibrium) is the bifurcation point (nonlinear buckling load). At the bifurcation point, B, the non-axisymmetric component of the total deformation has infinitesimal amplitude and its shape is the eigenvector, {q}, obtained from the eigenvalue problem:

$$[K1]\ \{q\} = \text{LAMBDA}*[K2]\ \{q\} \qquad (41.1)$$

in which [K1] is the stiffness matrix of the axisymmetrically deformed shell as loaded at the load step just before Point B (infinitesimally before B), LAMBDA is the eigenvalue, and [K2] is the "load-geometric" matrix corresponding to the difference in axisymmetric load states between that at the load step just before Point B and that just after point B. The post-bifurcation equilibrium path can be determined approximately by a new nonlinear analysis in which the shell has a very, very small initial imperfection in the shape of the eigenvector (buckling mode, q). The particular system shown above would exhibit very little or no sensitivity to initial imperfections, that is, the maximum load-carrying capacity and other behaviors would not strongly depend on the amplitude of the initial imperfection.

SHELL BUCKLING REFERENCES AND SHELL BUCKLING BIBLIOGRAPHY

See 1981pitfalls.refs.pdf and 1996bucklingsurvey.pdf and shellbucklingrefs.pdf .

PART 5:

A buckling failure that is not caused by an unavoidable imperfection, but is caused by a known flaw in the design. The design flaw can be thought of as an imperfection, but it is an "imperfection" that can be incorporated exactly into the analysis. Therefore, the shell is not "imperfection sensitive" in the "classical" sense of imperfection sensitivity in the presence of unknown and possibly random imperfections. The behavior of the shell with the design flaw is predictable if it is modeled correctly.

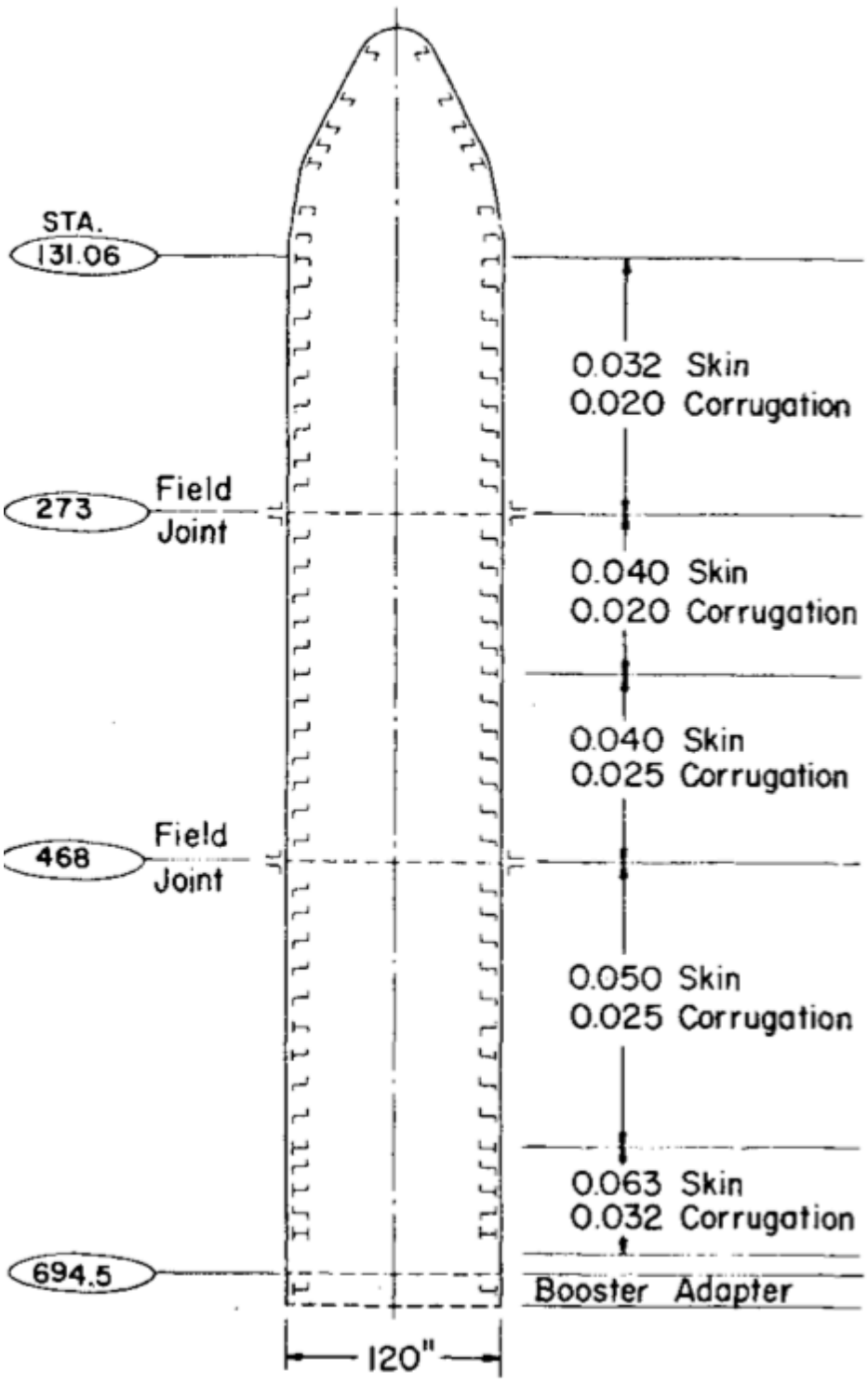

An externally corrugated, internally ring-stiffened payload shroud that failed during a test. The segmented stiffened payload shroud can buckle during launch. The skin thicknesses and external corrugation thicknesses (see Fig. 1.9b below) increase in steps from tip to base of the shroud. In a bending test of this payload shroud buckling occurred unexpectedly on the compressive side at the field joint at Station 468. As demonstrated in the next three slides, buckling can occur from non-axisymmetric external dynamic pressure that generates primarily axial compression on the leeward side of the shroud that increases from its tip to its base as the shroud bends like a beam under the non-axisymmetric dynamic pressure loading encountered during launch. (Fig. 1.9a in AIAA Journal, Vol. 19, No. 9, 1981)

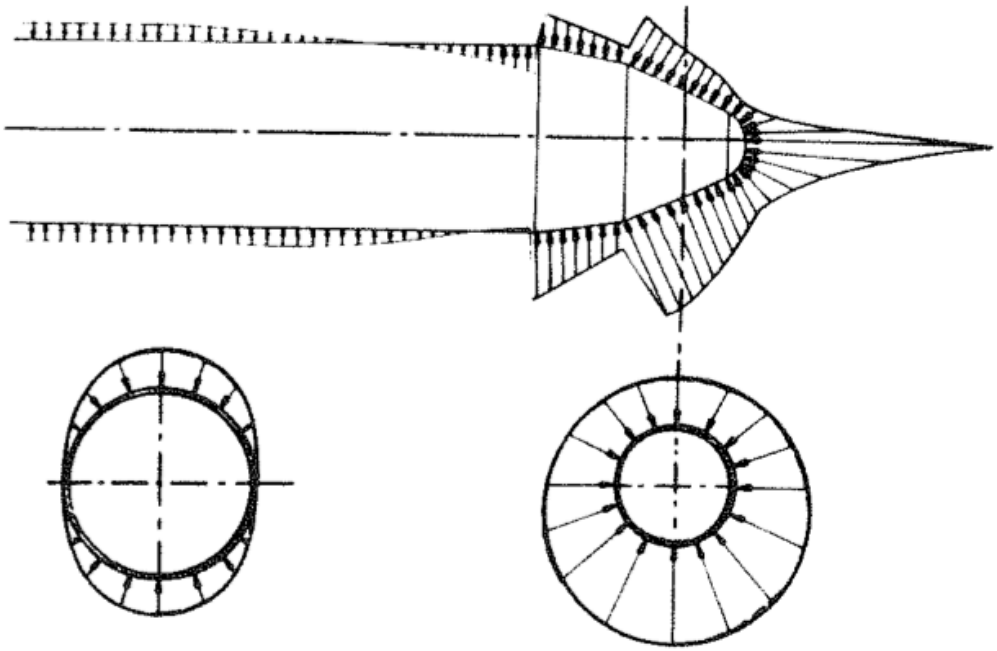

(a)

(b)

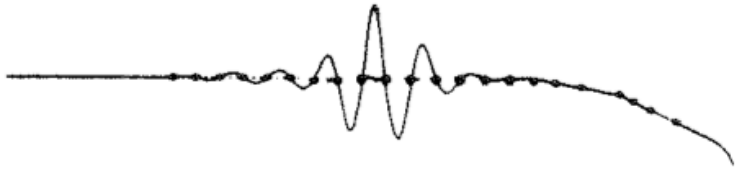

(c)

Slide 34 Buckling mode of a non-axisymmetrically loaded rocket payload shroud shown above in Fig. 9(a): (a) Pressure distribution measured in a wind tunnel test; (b) Pre-buckling beam-type deflection; (c) Non-axisymmetric buckling mode. Buckling is between the discrete rings and occurs with 13 circumferential waves. (from the PowerPoint file, pitfallsnasa.ppt). The BOSOR4 (BIGBOSOR4) computer program was used to obtain these results.

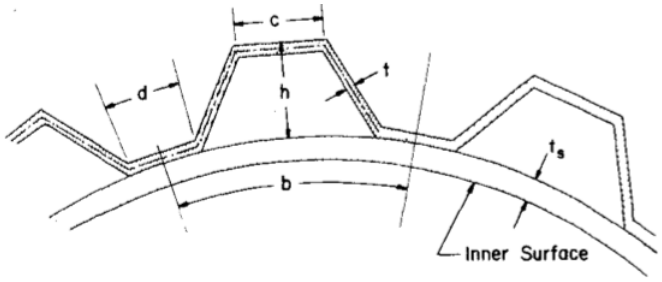

Fig. 1.9b in AIAA Journal, Vol. 19, No. 9, 1981
External axially oriented corrugations in the payload shroud.

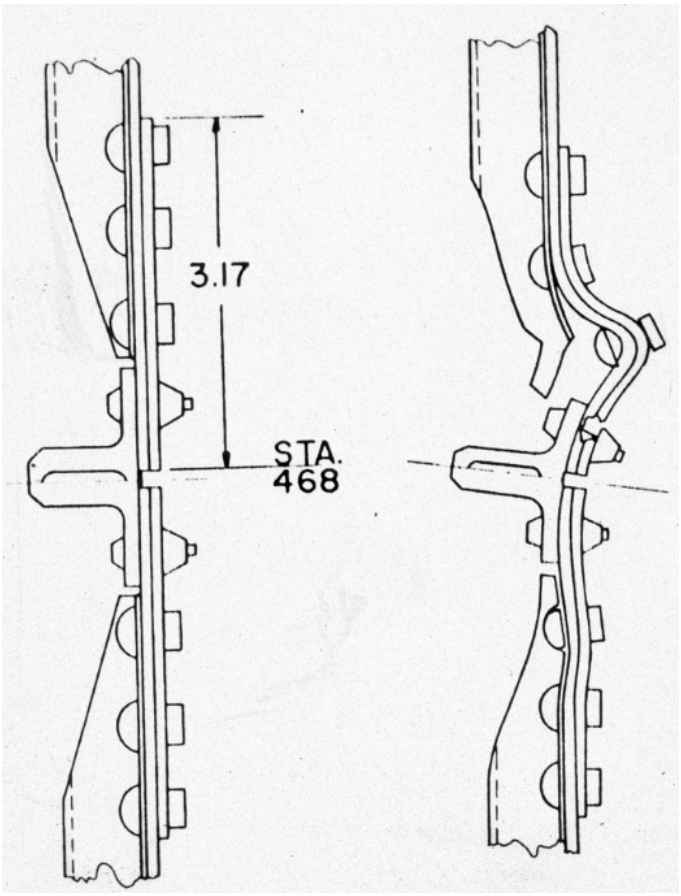

Fig. 1.9d in AIAA Journal, Vol. 19, No. 9, 1981
Schematic of local buckling failure at Station 468 in the payload shroud.

Fig. 1.9d (right-hand sketch above) Local buckling failure is caused by an axisymmetric inward excursion of the load path of the axial compression seen by the payload shroud at Station 478. This is a known “imperfection” that can be included in the computerized model. This known “imperfection” is the most serious imperfection in the entire fabricated shell because during a test the payload shroud failed because of it and not because of some unknown and unknowable random imperfection at some other location in the shroud. Therefore, one might say that the payload shroud as fabricated is not “imperfection sensitive” in the “classical” sense of that term. If the payload shroud had been designed taking account of the load path eccentricity at Station 468 (by the use of a thicker doubler, for example) then the stiffened cylindrical shell would be classed as “moderately imperfection

sensitive" (See Part 2 of the "page", imperfection sensitive). (Fig. 1.9d in AIAA Journal, Vol. 19, No. 9, 1981)

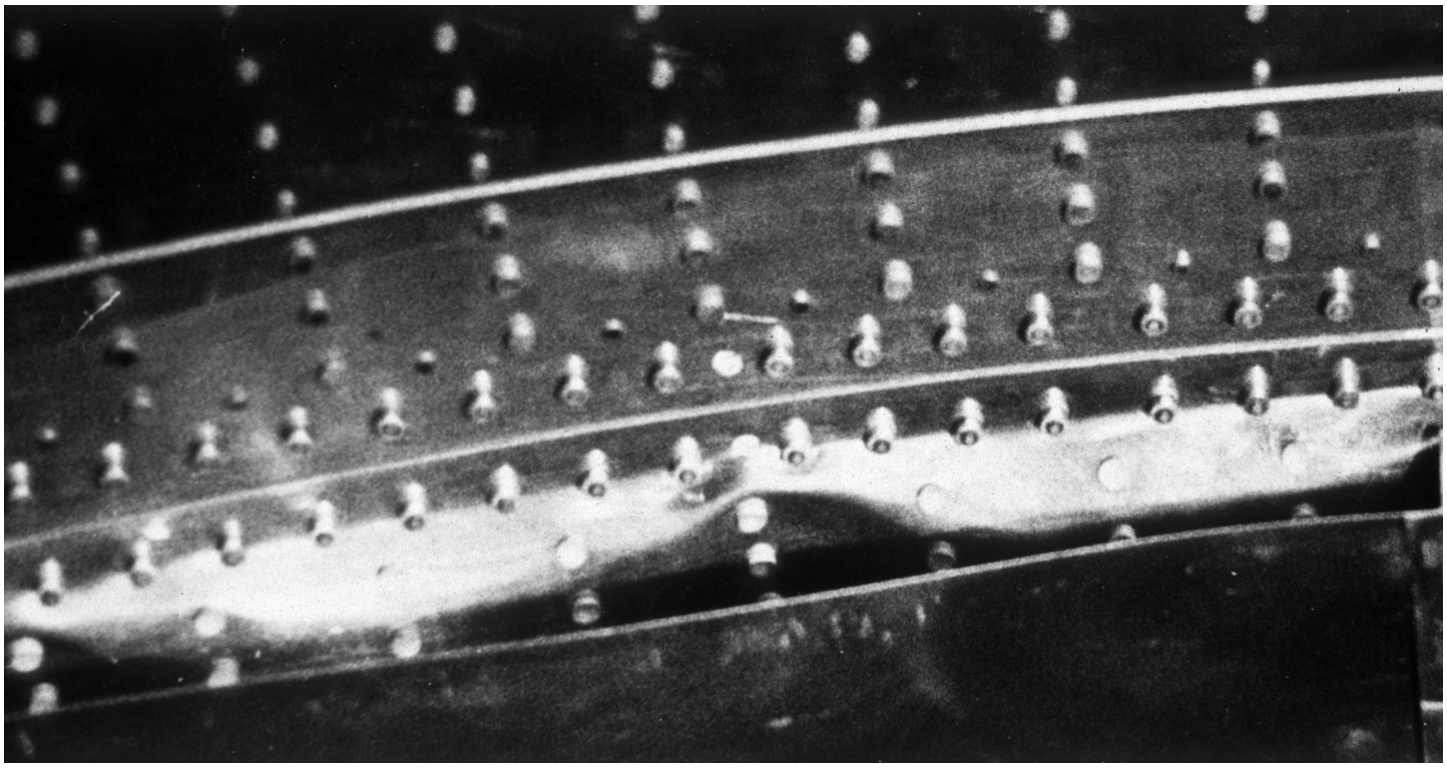

Fig. 1.9c Local buckling failure of the payload shroud at Station 468 that occurred during a test. (Fig. 1.9c in AIAA Journal, Vol. 19, No. 9, 1981)